

MODULATION INDUCING RETRODIRECTIVE
OPTICAL SYSTEM

Dr. Boyd Harned

26 COP

Technical Report
21 May, 1963 to 20 May, 1964

September 1964

Prepared For
NASA Headquarters
Washington, D.C. 20546
Attention: Code RET

Contract NASw-721(10-804)(10-1227)

GPO PRICE \$ _____
OTS PRICE(S) \$ _____
Hard copy (HC) \$ 3.00
Microfiche (MF) \$ 10.75

FACILITY FORM 802	N65-19864	
	(ACCESSION NUMBER)	(THRU)
	70	
	(PAGES)	(CODE)
	CR-57461	07
	(NASA CR OR TMX OR AD NUMBER)	(CATEGORY)

PHILCO.
A SUBSIDIARY OF *Ford Motor Company*
RESEARCH LABORATORIES
BLUE BELL, PENNSYLVANIA

MODULATION INDUCING RETRODIRECTIVE
OPTICAL SYSTEM

Dr. Boyd Harned

Approved by:

M. E. Lasser

M. E. Lasser
Assistant Director, Physics Laboratory

Technical Report
21 May, 1963 to 20 May, 1964

September 1964

Prepared For
NASA Headquarters
Washington, D. C. 20546
Attention: Code RET

Contract NASw-721(10-804)(10-1227)

ABSTRACT

19864

An investigation has been conducted into the feasibility of establishing an optical communications network making use of a passive modulation inducing device. The concept of MIROS, a Modulation Inducing Retrodirective Optical System, considers a passive element whose reflectivity changes in accordance with light of different frequencies and intensities so that the modulation of one beam is transferred within the element to another beam. Analytical and experimental studies have indicated that this system is feasible for long distance communication, using laser sources, and also that a number of techniques are possible. A rate equation analysis of a simple three-level scheme in a two-photon absorption process shows that the frequency response for cross modulation eventually falls off as ω^{-1} , but that the onset of this falloff may be shifted in frequency with the proper choice of the two beam intensities in comparison with the system relaxation time. Experimental investigations were concerned primarily with the production of amplitude modulation effects in optical pumping of cesium vapor, but the possibility of using the Franz-Keldysh absorption band edge shift in semiconductor materials was also demonstrated. Four methods of producing cross modulation with optical pumping were developed, spanning the electromagnetic spectrum from audio to optical frequencies. Application in low level satellites is discussed.

Author

PHILCO
A SUBSIDIARY OF *Ford Motor Company*
RESEARCH LABORATORIES
BLUE BELL, PENNSYLVANIA

CONTENTS

Section	Page
1. PURPOSE OF CONTRACT	1
2. NATURE OF CONCEPT	1
3. TECHNICAL DISCUSSION	2
3.1 Possible MIROS Mechanisms	7
3.2 MIROS Applications	14
3.3 MIROS Considerations	17
3.4 MIROS Design	18
3.5 MIROS Program	22
3.5.1 Technique of Optical Pumping	23
3.5.2 Technique of Band Edge Shift	37
4. CONCLUSIONS AND RECOMMENDATIONS	42
APPENDIX	Page
I SUPPLEMENTARY BIBLIOGRAPHY	I-1
II POWER REDUCTION FACTORS IN LASER TRANSMISSION FOR VARIOUS DISTANCES (r) AND BEAM DIVERGENCES (θ) CALCULATED ACCORDING TO $(r\theta)^{-2}$	II-1
III EDGE SHIFT DATA	III-1
IV FREE CARRIER ABSORPTION	IV-1
V THEORETICAL DISCUSSION OF OPTICAL PUMPING	V-1

LIST OF ILLUSTRATIONS

Figure		Page
1.	Retrodirective Optical System	1
2.	A Simple Three Level MIROS Scheme	5
3.	Light Transmission Change with Optical Pumping	13
4.	MIROS Intensifying System.	21
5.	Typical Optical Pumping System	24
6.	Examples of σ + Absorption and Nonselective Emission in Cesium to Show Optical Pumping.	26
7.	Cross Modulation By Varying Applied Magnetic Field Direction Variation of Signal as Frequency is Increased Maintaining Constant Coil Current	29
8.	Frequency Response in Optical Cross Modulation.	30
9.	Radio Frequency Case; Response of Optical Pumping System to Audio Modulated Zeeman Resonance Signal for Varying Carrier Frequencies.	31
10.	Microwave Case; Cesium Microwave Resonance, Frequency Response to Amplitude Modulation at Audio Ratios - 100 Percent Modulation Level (1000-ml Cell)	32
11.	Traces Showing AC Signals of Optical Pumping Beam and Electronically Modulated Cross Light Beam (DC) Signal	34
12.	Optical Pumping Transmitted Signal with RF-Zeeman Resonance Radiation; 43% Amplitude Modulated at 100 cps. Signal Generator Voltage and Audio Amplifier Gain are Indicated.	35
13.	Cesium Microwave Resonance, Response to Frequency Sweep at Audio Rates (1000-ml Cell).	36

LIST OF ILLUSTRATIONS (Continued)

Figure		Page
14.	Energy Diagram to Show Tunneling Mechanism With Applied Electric Field	38
15.	Sketch of Band Edge Modulator Fabricated at Philco.	40
16.	GaAs Edge Effect Modulator.	41

TABLE

Table		Page
1.	Maximum MIROS Range for Different Light Sources	15

MODULATION INDUCING RETRODIRECTIVE OPTICAL SYSTEM

1. PURPOSE OF CONTRACT

The purpose of the contract has been to investigate the feasibility of constructing a modulation-inducing reactive retrodirective optical system for application to space communications. Three phases of activity were outlined, as follows: (a) phenomenological collection and correlation, pertaining to the factors that determine the degree of interaction between two optical beams when incident on various media; (b) theoretical investigation of promising phenomena; and (c) experimental investigation of selected phenomena.

2. NATURE OF CONCEPT

As outlined in RFP No. SC-213, NASA, dated Jan. 14, 1963, "the quintessence of the concept is the transference of intelligence between two or more electromagnetic radiation beams without the consumption of auxiliary energy." The concept can be visualized by considering the remotely located retrodirective optical system, M of Figure 1, which receives light beams from two stations A and B, arbitrarily separated in distance, and redirects each beam to its sender. If one sender wishes to modulate his beam, the other sender receives the intelligence by means of the cross-modulation effects in the reflecting MIROS element. The passive nature of this element is considered to be of key importance, since an unattended system (in space, for instance) would be operative for decades.

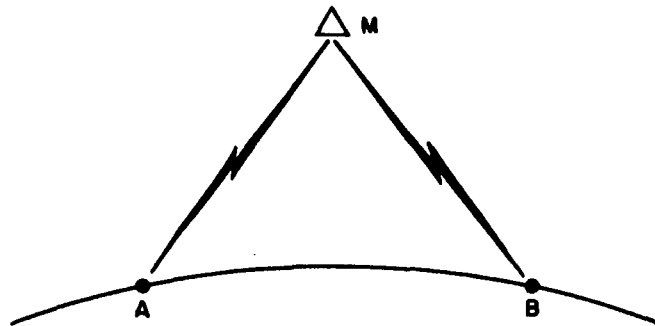


Figure 1. Retrodirective Optical System

3. TECHNICAL DISCUSSION

The nature of the problem suggests that the most desirable element is one whose reflection characteristics can be changed appreciably by the incident radiation, specifically when the two beams are incident simultaneously. Since transmission, absorption and reflection are conjugately related in radiation considerations, one may reduce the problem to that of finding a material with a variable transmission coefficient which is dependent on the presence of the two or more beams of radiation. To reduce the problem to its simplest form, one may consider an atomic or molecular system in which two photons are absorbed to produce the desired effect.

In outlining the requirements of the problem, it is instructive to consider quantitatively the nature of absorption in an atomic system. Mitchell and Zemansky¹ show that the absorption coefficient of a gas when considering only Doppler type broadening is given by

$$k_{\nu} = k_0 \exp \left[- \left(\frac{2(\nu - \nu_0)}{\Delta \nu_D} \sqrt{\ln 2} \right)^2 \right] \quad (1)$$

where $\Delta \nu_D$ is the Doppler breadth in frequency units which depends only on absolute temperature T and molecular weight M in accordance with the following:

$$\Delta \nu_D = \frac{2 \sqrt{2R \ln 2}}{c} \nu_0 \sqrt{\frac{T}{M}} \quad (2)$$

The factor k_0 is an ideal quantity representing the maximum absorption coefficient when Doppler broadening alone is present and may be expressed by the following two equivalent expressions:

$$k_0 = \frac{2}{\Delta \nu_D} \sqrt{\frac{\ln 2}{\pi}} \frac{\lambda^2}{8\pi} \frac{g_2}{g_1} \frac{N}{\tau} \quad (3)$$

-
1. Mitchell, A.C.G., and Zemansky, M. W., "Resonance Radiation and Excited Atoms," Cambridge University Press, 1961, Page 99.

$$k_o = \frac{2}{\Delta \nu_D} \sqrt{\frac{\ln 2}{\pi}} \frac{\pi e^2}{mc} N f \quad (4)$$

Actual situations which involve other types of broadening must be described by modifications of the above expressions, but, for our purpose, these equations qualitatively delineate our needs.

In expression (3) we find the factor N/τ , where τ represents a lifetime of the state to which an atom is excited when a photon of wavelength λ is absorbed. The factor N in the expression is the number density of atoms capable of absorbing such photons. The factor f in expression (4) is the oscillator strength of the transition in question, and for simple atomic resonance transitions is inversely related to lifetime.

In MIROS we have considered two-photon absorption processes as the only ones capable of cross modulating, as desired. Separate absorption events in pairs are assumed to take place in atoms or molecules. The second absorption event follows the first within the relaxation time of the atom and can take place only if the first event has taken place. The absorption coefficient of the second process may therefore be described in terms of the first. The first photon excites the atom to a higher energy state of lifetime τ in a process described by equation (3). The second photon adds more energy to the atom to excite it to another state of greater energy. It is desirable that this second state be of short lifetime and that the atom at this stage release its energy by radiation and return to the original state. Lifetimes of the states should be fairly long for the first and very short for the second. Oscillator strengths, by the same reasoning, should be small for the first absorption process and large for the second. This implies that the absorption coefficient of the first process will be poor unless the number density is large or linewidth small.

Reasoning tells us that we need to populate the first excited level at a high rate, and that we wish to keep these atoms excited for a fair length of time. Selection rules regarding quantum transitions tell us that we cannot have both of these features unless we introduce another quantum state. What is proposed as a desirable MIROS order of events is the following: (a) the first photon is absorbed to excite an atom to a very short lifetime state, allowing an initial high k_o ; (b) the atom relaxes, in some fashion, to another excited state of long lifetime; and (c) the second photon removes the atom from this second "metastable" state to some other very short lifetime excited state. These processes allow high absorption coefficients and fulfill our excited state lifetime needs.

Let us assume that this intermediate state can be qualitatively described by the absorption constant relations. The well-known equation

$$N = G\tau \quad (5)$$

describes the population of an excited state of lifetime τ in terms of its generation rate G . The generation rate for our metastable population will be given by the number of photons of type 1 absorbed, modified by the probability P that the excited atoms will relax into the metastable state:

$$N_2 = k_1 A I_1 dx P\tau / h\nu$$

where use is made of the relation $dI = -kI_1 dx$ in absorption, ($A dx$) being the volume element in question and $h\nu$ being the quantum energy per photon. Substitution of these quantities provide:

$$k_2 = \left(\frac{4 A I_1 dx}{h\nu_1} \right) \left(\frac{\ln 2}{\pi} \right) \left(\frac{\pi^2 e^4}{m^2 c^2} \right) \frac{N_1 f_2 f_1 P\tau}{\Delta\nu_{D_1} \Delta\nu_{D_2}} \quad (6)$$

Here the τ refers to the lifetime of the metastable state and the subscripts 1 and 2 refer to the two photon absorption processes. Although k_2 can be maximized in a number of ways, the most likely choice is a mechanism which will involve reasonably large f -numbers for a given incident intensity I_1 and Doppler widths $\Delta\nu_D$. The lifetime τ of the metastable state for practically any absorption mechanism probably depends, to a certain extent, on the number density of atoms N_1 ; further, one expects that the probability P of populating the metastable state is affected by N_1 variations. Expression (6) is applicable only in cases where resonance radiations are involved and Doppler broadening without complication from other broadening mechanisms may be assumed. However, we intend to make reference to its parameters when discussing other cases, keeping in mind the limitations of applicability.

Let us consider expression (6) in terms of MIROS. Two beams of radiation are incident on a material which can absorb energy from the beams. One of these beams is modulated, and it is desired that the variation appear in the transmitted energy of the other beam. Suppose beam (2) is modulated in amplitude. Our expression for k_2 accounts for a signal to appear on beam (1) through the population N_1 . The amplitude of this cross modulation with

frequency of variation of beam (2) will depend on the factors in our expression whose influence on N_1 may be frequency sensitive. The dominant parameter is seen to be the lifetime τ whose magnitude in comparison with the intensities of beam (1) and (2) will determine the populations N_1 and N_2 ; other parameters are not expected to vary with modulation frequency.

With regard to this frequency sensitivity, it is instructive to consider a simple three-level system² shown in Figure 2 below for the purpose of analytically describing the action. Level 1 with population N_1 absorbs radiation

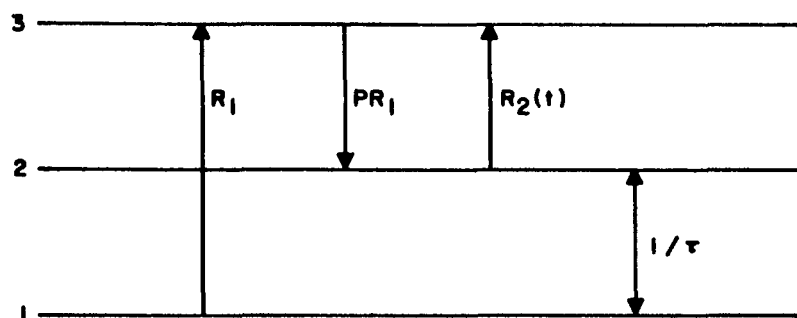


Figure 2. A Simple Three Level MIROS Scheme

from beam 1 at an unmodulated rate R_1 . Level 2 with population N_2 absorbs radiation from beam 2 at a modulated rate $R_2(t) = R_2(1 + m e^{i\omega t})$, where m represents a fractional modulation amplitude. Assume level 2 has a lifetime τ which will determine the length of time atoms stay in level 2 before reverting to level 1 by effects other than radiation from level 2. Level 2 is populated in accordance with the previous assumption that only a fraction

2. The theory which follows is similar in most respects to that presented by Dr. D. L. Carter of the University of Pennsylvania for MIROS optical pumping in our Monthly Progress Report #9, dated March 9, 1964. Somewhat more generality is gained in this treatment which shows the same type of result as Carter's set of equations which are in Appendix V.

of the N_1 atoms which absorb beam 1 reach our metastable state; i.e., PR_1N_1 , where P is our transition probability. Our simple rate equation is therefore:

$$\frac{dN_2}{dt} = PR_1N_1 - (R_2 + 1/\tau)N_2 \quad (7)$$

which becomes with $N_1 + N_2 = N$, the total number of atoms:

$$\frac{dN_2}{dt} = PR_1(N - N_2) - R_2(1 + me^{i\omega t}) + 1/\tau N_2$$

If now, one assumes a solution of the form

$$N_2 = N_2^0 + xe^{i\omega t} ,$$

substitutes this solution into the equation for dN_2/dt , separates the resulting equation into time dependent and time independent terms and into real and imaginary parts, the following solution is obtained:

$$N_2 = \frac{PR_1N}{\left(PR_1 + R_2 + \frac{1}{\tau}\right)} \left[1 - \frac{R_2 m \cos(\omega t - \Phi)}{\left[\left(PR_1 + R_2 + \frac{1}{\tau}\right)^2 + \omega^2\right]^{1/2}} \right] \quad (8)$$

where $\Phi = \tan^{-1} \left(\frac{\omega}{PR_1 + R_2 + \frac{1}{\tau}} \right)$, which represents a phase shift.

The fluctuation in N_2 with time is given by the second term of (8):

$$\Delta N_2 = \frac{-m PR_1 R_2 N \cos(\omega t - \Phi)}{\left(PR_1 + R_2 + \frac{1}{\tau}\right) \left[\left(PR_1 + R_2 + \frac{1}{\tau}\right)^2 + \omega^2\right]^{1/2}} \quad (9)$$

The assumptions require that variations in N_1 follow those of N_2 , since $dN_1/dt = -dN_2/dt$. Our signal, therefore, is proportional to (9) when we observe ac fluctuations of beam 1 in transmission. The rates R_1 and R_2 are determined by the absorptions of the two beams, and hence k_1 and k_2 . The signal is directly proportional to percentage modulation and is maximum when $m = 1$. The denominator in the above expression shows that a falloff in response is to be expected at sufficiently high frequencies of modulation, varying as ω^{-1} when $\omega \gg (PR_1 + R_2 + 1/\tau)$. For high frequency response it is therefore necessary that $(PR_1 + R_2 + 1/\tau)$ be made large, and this is most effectively done by making the intensity of beam 1 large. For the frequency region where $(PR_1 + R_2 + 1/\tau) \gg \omega$, the signal is proportional to $PR_1R_2 / (PR_1 + R_2 + 1/\tau)^2$, showing that the larger signals are obtained when lifetime is long and $1/\tau$ is negligible. If R_2 is proportional to τ , as (6) implies, then one of the best conditions for maximizing the signal is to make τ numerically about equal to PR_1 . For large fluctuations in N_1 , experimental observations must be made to determine the interdependency of the parameters. Application of the above analysis will be made later (in the report) to experiments performed in this laboratory using the technique of optical pumping.

3.1 Possible MIROS Mechanisms

In Philco Proposal R63-7, "Modulation Inducing Reactive Retro-directive Optical System," dated February 20, 1963, several possible systems were suggested for investigation. These were classified as:

1. Rare earth ions in lattices
2. Molecular excitations
3. Semiconductor effects
4. Non-stoichiometric crystals

In addition to these, work during the contract period suggested:

5. Optical pumping of alkali metal vapors
6. Photochromic materials

A brief description of specific processes involved will be given below. As a generalization, however, it may be significant to point out that many optical absorption phenomena can be used to perform the desired cross modulation experiments, and a large variety of physical states of matter

and regions of the spectrum may be involved. Quantum theory leads us to believe that wherever specific energy levels or bands can be identified in a material, these levels or bands can be used for the two photon processes we are discussing for MIROS application. Naturally, not all these processes are efficient. The problem of MIROS becomes, therefore, not so much one of finding a single mechanism which will do the job, but of selecting from the vast number one which can be exploited with reasonable power expenditure.

The first of the above mechanisms involves the same light pumping technique associated with pulsed crystalline lasers of the ruby type. Ions of doping material in crystalline or glass structure are excited to short life-time states by absorbing photons. Some of this energy is dispersed by the host material in radiationless phonon transitions, and the ions then find themselves in metastable states of lower energy but longer lifetime than the original. For MIROS, depopulation of the metastable states could be brought about by photons from a cross beam which would excite the metastable atoms to energy levels optically connected with the ground state. This double photon excitation has been performed experimentally with several materials. One excellent experiment is reported by Brown and Shand³ of triply ionized erbium in fluoride lattices. Other experiments have been done with praseodymium in fluoride lattices. In general the f-numbers of the absorptions are low, and high intensity sources are necessary. Erbium is interesting in that two infrared sources may be used, and the radiation emitted upon relaxation to the ground state is in the visible spectrum.

A number of gaseous species exhibit metastable excited states which are useful in a MIROS two-photon process. These long lifetime states, which are populated mainly by radiative transitions, are most commonly depopulated when atoms collide with one another. They may, however, be depopulated by photon absorption, as proposed here. One suggested gaseous MIROS example makes use of a metastable mechanism in mercury.⁴ Light of 2536 Å is used to excite ground state atoms to one level of a triplet state; collisions cause transitions of some of these atoms to the other two levels of the triplet state which are metastable. Excitation out of this metastable condition may be brought about by absorption of light of several wavelengths, most notable of which are the commonly used green-blue-violet triplet in the visible portion

3. Brown, M.R. and Shand, W.A., "Infrared Quantum Counter Action in Er-Doped Fluoride Lattices," Phys. Rev. Ltrs., 12, 367, 1964

4. Suggestion of Dr. H. Plotkin, mentioned in MIROS Progress Letter #1, 1963, to NASA Hdq., Washington, from Westinghouse Air Arm Division, Baltimore, Md.

of the spectrum. It is possible to have the same two-photon mechanism in gases useful for MIROS without having the first excited level metastable. A brute-force exciting technique without an intermediate process to bring atoms to metastability is required, as is seen from our $N = G\tau$ population equation, which tells us that power is inversely raised as lifetime goes down. Such a process was proposed for cesium;⁵ making use of one beam of resonance radiation to excite atoms from the ground state and the second beam of another wavelength to excite atoms to a higher energy state. An important point to consider in MIROS concerns the wavelength required to start the process of two-photon absorption. In gases the first excited state often lies at high energy above the ground state, corresponding to ultraviolet wavelengths which do not transmit well because of small particle Rayleigh scattering which varies as λ^{-4} . Thus, cesium 8943 Å radiation would be approximately 150 times better for long distance communication than the 2536 Å radiation of mercury of the same intensity. Atoms with two-electron spectra show metastable states which might be of use in a two-photon process. The Group IIB relatives of mercury - zinc and cadmium - are good examples; likewise, the Group IIA members which include calcium and barium. A choice of material from such a list depends on the wavelength of interest, the operating temperature to produce the correct vapor pressure and the relative ease in handling the material. Thus, for MIROS, an absorption bulb containing the material at the proper temperature for good absorption is subjected to resonance radiation from a source containing the same material. Some of the atoms which absorb are transferred from the resonance excited level to a metastable excited level through radiation or collision and are therefore receptive to photons from a second light source to remove them from this metastable level. The second absorption process is a short lifetime one and returns the atoms almost instantaneously to the original unexcited state so that the process may be repeated. Thus, the gaseous absorption process is similar to the crystalline one mentioned previously for MIROS, and the main difference in effect lie in the values of oscillator strengths and relaxation times in our absorption coefficients.

Absorptions in polyatomic species conceivably can produce the desired results for MIROS, and although they have not been investigated in detail, they will be mentioned here for completeness. Rotation, vibration and electronic excitations are observed in molecules, corresponding to extreme infrared, near infrared and visible-UV portions of the spectrum. For MIROS, the near infrared vibration spectra appear to be attractive from a wavelength

5. Proposal R62-166, Philco Corp., Nov. 6, 1962, to NASA Hdq. Washington, D. C., "Research on Semi-Passive Optical Repeater Components."

point of view. The two-photon process can be considered for molecules, as previously described for atoms, with the exception that only selected modes of vibration of the molecules are able to be excited. Metastable levels, as found in excited atoms, are not so readily identified in molecules because of the greater number of degrees of freedom and methods of dissipation of energy. Oscillator strengths are low for the same reason. It was originally proposed for MIROS to make use of combination frequency vibration bands in selected diatomic materials, one light beam being absorbed to excite one mode of vibration, and the second light beam being absorbed to further excite the material to another mode of vibration. However, because of the lower f-numbers and complex spectra of molecules, attention has been devoted mainly to the simpler atomic spectra.

Two semiconductor phenomena have been considered for MIROS application, the one involving photon absorption by bound charge and the other absorption by free charge which results from ionization. The latter process makes use of free carriers (electrons) in the conduction band of the lattice material; these carriers are observed to be very efficient absorbers of radiation in the near infrared region at about 10 microns. Free carriers may be produced by injection or bombardment of the lattice by particles or by optical (photon) absorption. For MIROS it was proposed that one of the two light beams be of small enough wavelength to produce free carriers, and the other be of long enough wavelength to be absorbed by the carriers. Detailed study of the process shows that free carrier production optically is not efficient, and the light intensity required would be prohibitive for long distance communication purposes.

The second semiconductor process proposed makes use of the Franz-Keldysh effect, which is concerned with an effective reduction of the energy gap between valence and conduction bands with application of an externally produced field. This band gap shift results in a displacement to longer wavelengths of the absorption band edge. The band edge, which is the wavelength or frequency interval over which the absorption falls from a large value to a small value, in some materials is as small as a few tens of Angstroms. If monochromatic radiation of wavelength just at the band edge is incident, switching of the electric field on and off can be made to produce an on-off effect in transmission of this monochromatic radiation through the material. Two techniques have been proposed for using the Franz-Keldysh effect in MIROS. One makes use of separate photovoltaic cells stacked in series to intercept light from one beam and build up the required electric field to cause variation in absorption coefficient of the semiconductor in question for the second beam. The other scheme is to combine the two "cells" into one package by making use of two layers of different doping, separated by

a p-n junction across which the required electric field exists. An electric field exists across the junction in darkness, because of diffusion of charge; the value of this field is given approximately by the ratio of gap energy to depletion region thickness. Photons of energy equal to or greater than the gap energy can be absorbed and create charge pairs. Thus, exposure to radiation causes absorption which tends to reduce the junction field because of flow of charge created by the absorption. A second beam's radiation of wavelength just longer than that corresponding to the "dark" conditions will not be absorbed until radiation of the first beam is absorbed to cause a reduction of the junction field. Modulation of the first beam will appear in the transmitted intensity of the second beam if field conditions are chosen properly to allow partial transmission of each beam simultaneously.

Another solid state MIROS process which depends on motion of charge in a lattice is that of photon absorption by color centers in non-stoichiometric crystals. These color centers are commonly produced in alkali halide crystals by bombarding with high energy photons, and one type produced is the F-center which is accepted to be a halogen ion vacancy site where an electron is loosely bound. These electrons can be liberated by irradiation of the crystal with light in the visible range, and they can be caused to drift in the lattice when an electric field is applied. These electrons can be trapped in other F-centers, so that two electrons are bound at one vacancy site, thereby forming F'-centers. The F'-centers may be reconverted to F-centers by irradiating with light of the proper wavelength, usually of lower energy than the F-center wavelengths, thereby constituting a reversible process suitable for MIROS cross modulation work. Drift velocities of the electrons are dependent on crystal temperature, and modulation capabilities, in terms of frequency response, are therefore temperature sensitive. Conversion efficiencies are very good, and oscillator strengths associated with the absorptions are also very high. The process can be performed with a large choice of monochromatic radiations, since the absorption bands of the color centers are usually broad. The most efficient operation in converting from one to another of the color centers appears to be about -140°C . Room temperature operation is possible, but efficiency of trapping into the F'-center, because of the low binding energy, is quite poor. Actual drift of the electrons away from the F-center should be aided by application of the electric field, and this cannot be done in a passive device except as previously mentioned with photovoltaic cells.

Another mechanism which has been considered, but not investigated in detail, is that of photochromism which has to do with the change of transmission properties of a material when subjected to light of varying intensities.

Increased work in the field recently has shown that a number of materials can be used for such effects, both in increasing and decreasing of transmission when irradiated with light of a particular wavelength. For instance, a sodium silicate glass doped with either Ce^{3+} or Eu^{2+} ions has an absorption band centered at about 3200 \AA which causes changes in transmission for wavelengths in the visible spectrum. The explanation of the effect is in the creation of color centers similar to the F-centers of alkali halide crystals, significantly different from the alkali halides because of the relatively low energy photons required to liberate the electrons which are trapped to form the centers. Relaxation of the centers occurs in times varying from microseconds to seconds, and the process is reversible, as would be required in a MIROS application. Organic compounds are known to become opaque to visible radiation in microsecond times when exposed to light from an electronic flash and regain transparency in cyclical operation. Certain colored glasses containing compounds of selenium and cadmium sulfide have been shown to increase transmission for a particular wavelength (ruby laser line) with high intensity exposure and have recently been used in nanosecond Q-switching of crystal laser sources. The variations in transmission of these materials are most noticeable when the intensities are very high, and long distance communication making use of them would require extremely intense sources.

The final example to be mentioned in this section of physical processes possibly applicable to MIROS needs is one which has received the most attention, both analytically and experimentally, in this laboratory. This is the technique of optical pumping of alkali metal vapor, by which the population of certain magnetic sublevels of ground state atoms is varied and causes variations in the monochromatic transmission coefficient of the vapor. If one observes such a system from switch-on time, transmission of light to a photodetector through an absorption bulb will be found to increase from an initial level to a final level with a time constant proportional to pressure, temperature and constituents in the bulb. See Figure 3, where T_1 is transmission without optical pumping, T_2 with pumping after a magnetic field is turned on at t_0 . Apparatus required to observe the effect includes a light source of the proper wavelength, filters to render the light monochromatic and circularly polarized, an absorption bulb containing vapor of the material to be pumped, coils or a permanent magnet to provide a magnetic field at the bulb whose direction is along or opposite to the light propagation path, and a photodetector. Without the magnetic field each component of the doublet ground state of the alkali metal atoms has its magnetic sublevels superposed and indistinguishable. The magnetic field causes separation of these levels and restricts quantum mechanically the number of ways any given atom can absorb radiation because of angular momentum considerations. When the incident light is circularly polarized, the absorption possibilities of an atom

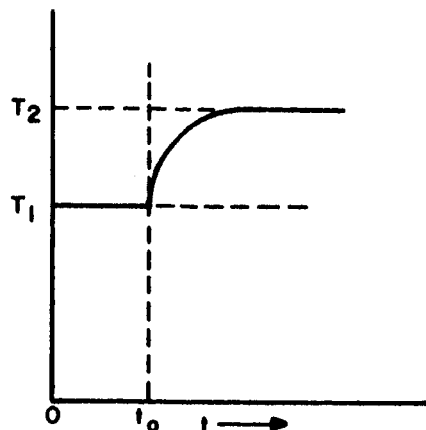


Figure 3. Light Transmission Change with Optical Pumping

are further restricted. Those atoms which do absorb reradiate their energy in about 10^{-8} sec through spontaneous emission and return to ground state magnetic sublevels which may be different from the originals. Normally the populations of these ground state sublevels are about equal, as would be the case at switch-on time. The result of optical pumping is an aggregation of atoms into a high population of one of the magnetic sublevels from which absorption of the pumping photons is not allowed. If conditions are properly chosen atoms can return to this level from an excited state but cannot be removed from it by absorption if an excited state to which the atom could be raised does not exist. Thus, for pumping photons incident on an absorption bulb, atoms in all ground state magnetic sublevels but one, will absorb, be excited to a resonance state and immediately revert, through spontaneous emission of the absorbed energy, to the same or another ground state level. The one level which did not absorb may be increased in population and cause the number of absorbing atoms to decrease. Since all incident photons effective in pumping are of the same energy, the percentage transmission of light will increase as the population of this level is increased. Atoms are removed from this "pseudo"-metastable level by collision processes which tend to change the energy or angular momentum value or by absorption processes which are quantum mechanically allowed. The collision process is one which determines the lifetime τ of the level. Absorption by these "pumped" atoms can only take place if a second source of radiation is present with photons of another wavelength or state of polarization.

This optical pumping process therefore constitutes the kind of system mentioned earlier as desirable for MIROS needs. A metastable level is available into which atoms can be driven by one light source and from which the atoms can be removed by a second light source. This alkali metal atomic metastable level differs from other metastable levels we have discussed in being a low lying level in energy. It actually is one of the ground state levels whose excitation energy is not permanently fixed, since it is arrived at by Zeeman (magnetic) splitting; it therefore can be slightly moved in the energy spectrum, a convenience which allows fine tuning to be performed. Atoms finding themselves in this level can absorb photons corresponding to resonance energies to remove themselves from the level, and these energies are spread in the radiofrequency, microwave and optical portions of the spectrum over narrow ranges which depend on strength of the applied magnetic field which causes the Zeeman splitting. Hence, MIROS demands can be satisfied in optical pumping not only with optical frequencies but also with radio and microwave frequencies, and it is with experiments of this kind that the Philco MIROS program has devoted its attention.

3.2 MIROS Applications

A successful retrodirective optical system capable of cross-modulating two light beams undoubtedly will find its main use in a satellite system, but other applications are also suggested. Remote marine or mountain locations of the MIROS element are possible for short distance transmissions where other means of communication may not be possible. One can visualize a MIROS communications system finding use in explorations of other planets. In any case, the MIROS element is conceived as unattended and remaining relatively fixed in position with respect to the locations of the two or more transmitting stations involved in the network. The 24-hour synchronous satellite is assumed in this report to be the most desirable location for the MIROS element because of its fixed direction and distance from a terrestrial sender.

The main failing of optical communications networks will probably always be the problem of attaining high transmission intensities, in spite of rapid laser development to date. As stated earlier, our MIROS investigation has in reality been one of ascertaining an efficient process. For a given intensity a large number of processes might be used to carry on intelligence exchange, provided that the distances are not large. It would be convenient to classify processes in terms of the distance they could be used in such a communications network, whether it be across the laboratory or across the country via high altitude satellites. Unfortunately, this method of classification has not been

done; the many unknown factors of these quantum processes restrict our judgments to generalities.

Let us consider the laser source as the transmitter in our MIROS network. Because of the coherence properties of such sources, they are capable of producing very small beam divergences, limited only by diffraction effects. One can therefore transmit optical power over long distances without excessive losses, as has been shown on numerous occasions. A factor of importance in determining usefulness of a given source for MIROS is the detector sensitivity; i.e., receptiveness to any of the retrodirected photons. Since all beams diverge at some minimum angle, say α , the power incident per unit area at a distance R will be reduced by a minimum factor of about $(R\alpha)^{-2}$. For MIROS, where out-and-back transmission is required, one may consider the reflector to act as a second source which returns the power degraded by another factor of $(R\alpha)^{-2}$. Therefore, the minimum power required is $SR^4\alpha^4/A_rA_c$, where S is the detector sensitivity and A_r and A_c are the areas of the reflector and collector. The maximum distance R at which a given source of power P_o can be used is therefore given by $(A_rA_cP_o/S)^{0.25}\alpha^{-1}$. Let us assume that S is about 10^{-14} watts and both A values are 100 cm^2 so that an estimate of distances R may be made for various beam divergence angles and source power values.

TABLE I
MAXIMUM MIROS RANGE FOR DIFFERENT LIGHT SOURCES

α P_o	1 sec	10 sec	100 sec	1000 sec
1 watt	$6.3 \times 10^9 \text{ cm}$ $3.9 \times 10^4 \text{ mi}$	$6.3 \times 10^8 \text{ cm}$ $3.9 \times 10^3 \text{ cm}$	$6.3 \times 10^7 \text{ cm}$ $3.9 \times 10^2 \text{ cm}$	$6.3 \times 10^6 \text{ cm}$ $3.9 \times 10^1 \text{ mi}$
10 watts	$1.12 \times 10^{10} \text{ cm}$ $0.7 \times 10^5 \text{ mi}$	$1.12 \times 10^9 \text{ cm}$ $0.7 \times 10^4 \text{ mi}$	$1.12 \times 10^8 \text{ cm}$ $0.7 \times 10^3 \text{ mi}$	$1.12 \times 10^7 \text{ cm}$ $0.7 \times 10^2 \text{ mi}$
100 watts	$2 \times 10^{10} \text{ cm}$ $1.24 \times 10^5 \text{ mi}$	$2 \times 10^9 \text{ cm}$ $1.24 \times 10^4 \text{ mi}$	$2 \times 10^8 \text{ cm}$ $1.24 \times 10^3 \text{ mi}$	$2 \times 10^7 \text{ cm}$ $1.24 \times 10^2 \text{ mi}$
1000 watts	$3.56 \times 10^{10} \text{ cm}$ $2.2 \times 10^5 \text{ mi}$	$3.56 \times 10^9 \text{ cm}$ $2.2 \times 10^4 \text{ mi}$	$3.56 \times 10^8 \text{ cm}$ $2.2 \times 10^3 \text{ mi}$	$3.56 \times 10^7 \text{ cm}$ $2.2 \times 10^2 \text{ mi}$

Now, since 10 seconds of arc divergence of a laser beam is about the best we can expect in present technology, it appears that the minimum power we can tolerate for a 24-hour satellite is about 1000 watts for detectivity at the receiver. This represents about $0.04 \text{ microwatts/cm}^2$ at the MIROS element. We are curious to know if this is sufficient to satisfy the needs of the MIROS mechanism. As an example of one system, consider the case of optical pumping. The number densities of atoms in the gaseous vapors used in optical pumping are typically $10^{10}/\text{cm}^3$, and lifetimes of 10^{-3} seconds may be assumed. Using our equation (5) which states that $N = G\tau$, we find a generation rate of about $10^{14}/\text{second}$ is required if we assume a 10% efficiency, and this corresponds to a power density of $20 \text{ microwatts/cm}^3$ at 0.9μ photon wavelength. This level is considerably above the minimum calculated above, but an efficient collection system at the MIROS element could provide the correct level within a small volume. It must be remembered that optical systems and atmospheric propagation are not 100% efficient, and the minimum tolerable transmission intensity therefore probably lies 50% or more over that calculated.

It would be certainly advantageous if the MIROS element could respond to small power and not require a photon collection system at the satellite. At this point in our investigation we should like to know if the photon density quoted above for optical pumping is typical for two-photon systems and represents therefore an efficient mechanism. Measurements of optical pumping powers in Philco laboratory experiments have shown that the range 1 - 100 microwatts/cm² is normally attained and is sufficient for demonstrating cross modulation action. The value of $0.04 \mu\text{watts/cm}^2$ incident at a 24-hour satellite was calculated by assuming a sensitivity for a given detector, and a less sensitive detector would make our case more pessimistic.

As means of approaching the problem of MIROS sensitivity, let us consider briefly the problem of detector sensitivity. In their book on detection of infrared radiation, Smith, Jones and Chasmar⁶ consider the problem of minimum detectable power for thermal and quantum detectors in terms of fluctuations in radiation and flow of charge in circuits. The minimum detectivity in MIROS elements is analogous to that of quantum detectors with the added complication that two quantum processes must be considered. The minimum radiant power that a detector can see amounts to the amplitude of the radiation fluctuations modified by the quantum efficiency of the detector. A similar case holds for a MIROS element, for we are seeking modulation on

6. R. A. Smith, F. E. Jones and R. P. Chasmar, "The Detection and Measurement of Infrared Radiation," Oxford Clarendon Press, 1957, p. 280.

small signals which, in the limit of small power, will appear similar to thermal and radiation fluctuations. We may therefore borrow from the theory of detectivity to estimate the power levels required.

Let us consult a list of typical detectors⁷ for ranges of sensitivity. For optical pumping of cesium, a wavelength of 8943 \AA has been used. An example of a good room temperature solid state detector for this wavelength is the 1N2175 silicon photoconducting duo-diode. This is listed as having a noise equivalent input of about $4 \times 10^{-11} \text{ watts/cm}^2 (\text{cps})^{1/2}$, measured at 400 cps, with an optimum chopping frequency of 20 kc/sec at a response time of about $8 \mu\text{sec}$. The above numbers and units tell us that detectors are rated in terms of power/area-bandwidth, and specified for a given frequency and operating temperature. If we wish to translate this detector information to MIROS terms, we must consider the fact that wide band communication is desired and the numbers must be modified by the square root of the bandwidth and contain factors which account for quantum efficiency and spectral response. Considering all these factors and the $10^{-11} - 10^{-12} \text{ watts/cm}^2 (\text{cps})^{1/2}$ detector sensitivities, we are inclined to estimate $10^{-7} - 10^{-6} \text{ watts/cm}^2$ sensitivity as good for a MIROS element for bandwidths in the audio and low ultrasonic ranges. By the same token, we admit to a possible self deception in the example above where a power of 10^{-14} watts was received. Minimum detectable powers of the returning beams involving large bandwidths appear therefore to require much higher transmission powers than previously calculated, and this in turn could lead to higher calculated power at the satellite, possibly making it unnecessary to consider the use of an optical collection system.

3.3 MIROS Considerations

Long distance communications impose several requirements on our passive MIROS element, among which are the following:

- a. Good modulation frequency response, implying short lifetimes of energy states involved in the two photon processes. A one-millisecond lifetime implies kilocycle/second response, and microsecond lifetimes imply megacycle/second response.
- b. High absorption coefficients for both beams of the radiation involved so that efficiencies and signal levels will be high for easily fabricated geometries.

7. For instance, "Elements of Infrared Technology," P. Kruse, L. McGlauchlin R. McQuistan, John Wiley and Sons, New York, 1962, p. 420.

- c. Ability to operate at low power levels of high efficiency, as the information on power reduction, generation rate and lifetime above indicates.
- d. Selective in frequency in the presence of other radiation sources to avoid the use of complicated filtering action which tends to reduce available power; atomic processes with pass-bands less than one Angstrom unit appear to be preferable.
- e. Ability to handle high rates of intelligence without distortion; some, if not all, of the proposed MIROS processes involve phase shifts which depend on modulation frequency, and some appear to be nonlinear in intensity response.
- f. Insensitive to hazards of space travel, including temperature variation and exposure to extraneous photon and particle bombardment.
- g. Ability to transfer modulation from any one beam to another if two or more beams are incident simultaneously. It is desirable that each sender be made aware of the presence of the beam of other senders through variations in absorption of his own beam. Some methods proposed are not sufficiently sensitive enough to allow this possibility, particularly those whose exciting efficiency from the ground state is low.

3.4 MIROS Design

The above considerations tend to limit design possibilities of the MIROS element if it is to be used in space work as a passive device. As is so frequently the case in the fabrication of a system to demonstrate a principle, compromise is necessary to conform to existing techniques and materials, and the realization of all desirable attributes of a MIROS network is beyond doubt an elusive goal.

Consider the retrodirective optical system. We should like to inquire into the nature of a reflecting element which will return radiation as exactly as possible without deflection to its origin with minimum losses. Simple geometrical optics tells us that we should use parallel light with collecting areas equal to, or greater than, the area used at the sender to render the light parallel. The reflector is undoubtedly chosen universally as a corner reflector, whose ineluctable retrodirectivity, regardless of incidence angle over a wide range, makes this type of reflector superior to other types

which have to be carefully aligned. Curved surfaces, of course, are possible but must be used in combination in order to avoid annoying deflections and beam spreading. Let us assume that our retrodirective element is the corner reflector. This can be a simple three-sided mutually perpendicular corner or may take the form of a transparent solid, crystalline or glass, with internal reflections. The question of greatest interest is how we can most effectively use our choice of MIROS material with one of these retrodirective elements. Following are possible means:

- a. The corner reflector made up of highly reflecting plane sides mutually perpendicular with:
 1. The active element embodied in sheets overlaid so that the radiation makes two passes through the modulation inducing material.
 2. The active element contained in an absorption cell, as a vapor, for instance, contained in the volume formed by the three sides.
 3. Enclosure of the volume formed by the three sides into a tetrahedron by means of transparent cover material so that the corner reflector volume itself contains the MIROS material without the need for a separate absorption cell.
- b. The corner reflector sides make up the MIROS material, as a semiconductor, for instance, so that the reflectivity coefficient of the reflector is a function of the incident light.
- c. A collecting lens system mounted in front of the corner reflector which first condenses incident radiation to a small volume for intensification purposes and then renders the light parallel before reflecting back through the system from the corner reflector. This double pass scheme allows the MIROS absorption cell to be placed at the focal region of the first lens and offers a means of using extremely small area (or volume) units such as band edge shift modulators.

Let us consider briefly the nature of the corner reflector in its ability to reflect radiation. Reflection of a ray by the three mutually perpendicular sides of the corner (three reflections) takes place in such a fashion that the ray is exactly reversed in direction but displaced laterally from its original path. The image of an object seen in the reflector is reversed, right for

left and up for down, as might be expected from the lateral displacements. A parallel beam will be reflected with the same degree of spreading. If a beam diverges, one finds by simple geometrical construction that the rays reflected in reverse direction to arrival do not describe a beam whose divergence has decreased. In other words, a divergent beam continues to diverge after reflection from a corner reflector. If, however, a slowly divergent beam strikes an array of closely spaced corner reflectors, one finds that a very high percentage of the incident light is returned to the sender, each element intercepting only a small portion of the divergent beam and tending to treat the wavefront as parallel. Such an array has already been nicely designed and fabricated for the S-66 Satellite.⁸ Since fabrication of such reflectors cannot be perfect and is made to a specification of divergence angle α_r , our formula for minimum power must be modified by the factor $\left(\frac{\alpha_r}{\alpha_s}\right)^2$, where α_s is the divergence angle of the sender. The S-66 corner reflectors have a divergence angle of 20 seconds, twice that of our 10-second sender, giving an increase of a factor of 4 in minimum power required in our examples.

Suppose we consider the 20 microwatt level estimated for optical pumping as a typical incident power/cm² required in a MIROS network. If a source of a kilowatt power output, 10 seconds divergence angle, is used for the 24-hour satellite, we know that about 500 times this intensity is needed, and we are forced to use some kind of auxiliary optical system to condense the light. The lens pair combination mentioned previously with a corner cube array can be used for this purpose, one lens used to focus light and a second identical lens located so as to make the transmitted light parallel again before being reflected from the corner cube. Each corner cube of the array would have its own lens pair. Lenses of F-number unity and diameter 2.5 cm produce a power intensification of coherent light numerically equal to about λ^{-2} , or 10^8 for 1 micron wavelength radiation, far exceeding the amount required. The volume over which the power density between the two lenses is equal to or greater than that required depends on the focal length of the lens but probably would not exceed 1 cm³ for a practical system.

The above example indicates one possible design criterion which is difficult to avoid. This is the need for a small volume MIROS element which may effectively be placed near the focal plane of a collecting optical component. In other words, it appears that an array of corner cubes is imperative in order

8. Plotkin, H. H., "The S-66 Satellite Tracking Experiment," Quantum Electronics, III, Proceedings of the 3rd International Conference, Edited by P. Grivet and N. Bloembergen, Columbia Univ. Press, 1964, p. 1319, Vol. II.

to receive appreciable reflected intensities. Unless extremely high transmitted power is used, each corner cube should be fitted with a collecting lens system to increase power level at the MIROS element. Geometry dictates that the MIROS element be of small cross-sectional area and small volume, of the order of a few millimeters rather than centimeters. The total number of corner cube elements required to provide a detectable signal at the sender's location can be estimated from $A_r/A_q\eta$, where A_r is the estimated reflector area, A_q is the area of an individual corner cube and η is an effective efficiency of reflection by any one corner cube-lens pair combination. It is doubtful that η could exceed 0.5 because of losses at surfaces and vignetting in off-axis incidences. The S-66 corner cubes have about 5 cm^2 surface area; a required $A_r = 100 \text{ cm}^2$ with $\eta = 0.5$ would therefore set a minimum number of corner cubes at 40 in the line of sight of the sender. It is interesting to note (Ref. 8) that the S-66 provides for 8 trapezoidal panels with 40 corner cube elements on each panel. A similar arrangement appears to be advisable for MIROS requirements.

There is a possibility of very low efficiency in the use of an optical system for intensifying the collected radiation which the MIROS element sees.

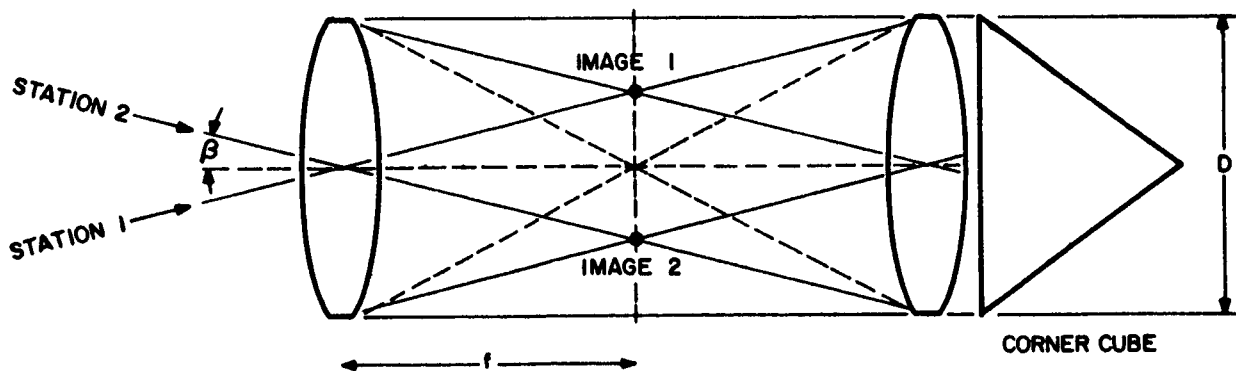


Figure 4. MIROS Intensifying System

Ray tracing through the lens pair (see Figure 4) shows that the maximum off-axis angle allowable for the second lens to intercept one half the radiation

and return it to the sender is given by $\tan \beta = (4F)^{-1}$, where F is the F -number of the lenses. This angle for an $F/0.5$ lens is 26.5° and is 2.9° for an $F/5$ lens. The total angle (2β) desired for the retrodirective system in MIROS for a 24-hour satellite should be about 20° , and this can be accommodated with an $F/1.4$ lens pair. A further complication arises, however, because the images from two earth stations separated by this subtended angle (2β) are displaced in the focal plane of the first lens by $1/2$ lens diameter. Since most two-photon MIROS mechanisms require that the two exciting light beams be fairly well superimposed on the active volume of the MIROS element, the lens collecting system is limited further in acceptance angle depending on the amount of carrier diffusion which can be expected in the MIROS element. Gaseous MIROS elements, such as in optical pumping, are most effective in this regard. This image displacement would be worse for low altitude satellites than for a synchronous one because the angle subtended by two fixed sending stations would be larger.

Some of the above considerations make the design of a MIROS satellite somewhat complex. The simplicity of the S-66 satellite is desirable but not attainable unless the MIROS element can actually be constructed in the form of a corner cube. Several alternate shapes are suggested for accommodating a larger number of corner cubes, among which are (1) the three mutually perpendicular planes making up a corner, (2) the frustrum of a cone or pyramid, or (3) a regular polyhedron. Addition of a condensing lens system complicates the structure by requiring mounting frames. Temperature stabilization probably will be required for any choice of MIROS element, and this is assumed to be possible by appropriate selection of material and design of the satellite so that the albedo may be "tuned." If filters or anti-reflection coatings are required on the MIROS components, some difficulty may be encountered in temperature control. The technique of optical pumping requires the presence of a magnetic field at the absorption unit, and this is easily obtained for one cell by use of a horseshoe magnet. When a large number of cells is used, each with a corner cube, the magnetic field can be obtained by bar magnets located behind the corner cubes. Exact design depends, of course, on the stability requirements of the satellite, whether magnetic or not, and the degree of interaction of such a system with the earth's magnetic field.

3.5 Philco MIROS Program

At the start of the contract period Philco had already begun a small experimental investigation of the possibility of cross modulating two light beams within an optically pumped absorption cell. Equipment which had been collected for another purpose was found to be more appropriately devoted to MIROS needs. Therefore, when it was found relatively easy to obtain a modulated

signal with the technique, more and more effort throughout the program was expended, first, to improve the signal, and, secondly to explore and compare the several possibilities of performing the modulation with the optical pumping apparatus.

In addition to this effort, and in conformance with terms of the originally proposed program and contract, a study program was initiated and maintained throughout the contract period. Several MIROS mechanisms were considered in varying degrees of detail, and one of these was found interesting enough to be investigated more thoroughly experimentally. This is the technique of absorption band edge shifting through electric field variations.

The experimental programs were aimed primarily at demonstrating the feasibility of a MIROS approach, rather than at measuring limiting values for system use. Experimental apparatus, therefore, was more of the "breadboard" type and was useful in showing areas requiring the most development. Although a small effort was spent to set up the retrodirective type experiment, making use of a corner cube and beam splitting equipment, most of the experimental effort was devoted to the more elementary laboratory bench (short distance) optical paths.

Details of the two experimental programs are presented in following sections. Recommendations of the program have to do with these two MIROS techniques, and these are discussed in the final section of this report.

3.5.1 Technique of Optical Pumping

In order to explain more fully the versatility of the optical pumping technique and to present the quantitative information obtained in this contract work, the following detailed explanation of cesium resonance transitions is included.

The apparatus required for observation of optical pumping is very simple, and only elementary laboratory procedures are required for operation. Although the mechanism described is that of pumping of cesium vapor it should be borne in mind that all alkali metal vapors can produce similar results for their own peculiar temperature and wavelength conditions. A source S in Figure 5 emitting radiation at the cesium resonance frequencies has its radiation collimated by lens L_1 through a filter combination $P_1 - P_2 - F_1$ into cesium vapor contained in an absorption cell, and the transmitted light is collected by lens L_2 and passed through filter F_2 to a photodetector. The filter combination consists of an interference filter, a linear polarizer and a retardation plate for rendering the light "monochromatic" (a narrow pass band)

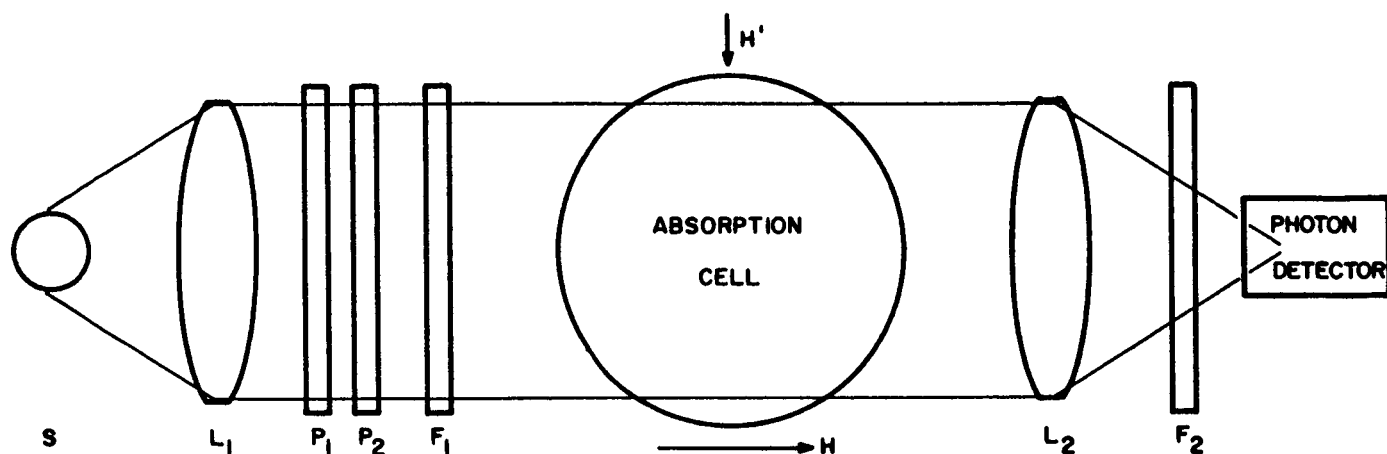


Figure 5. Typical Optical Pumping System

and circularly polarized. Filter F_2 is tuned to this wavelength and is included only to maximize response by eliminating unwanted radiation at the detector from other sources. An axial magnetic field H is applied to produce the desired effect, and the presence of any other field H' tends to reduce it.

The cesium resonance radiation is absorbed in part by the atoms of the absorption cell. The existence of the magnetic field H and the state of polarization of the incoming radiation restricts the manner in which the absorbing atoms can become excited through photon absorption. In magnetic fields atomic energy levels undergo Zeeman splitting, and monochromatic absorption or emission of radiation is observed to occur at a number of new frequencies when the splitting takes place. For cesium the first excited state $^2P_{1/2}$ lies at an energy level corresponding to 8943.5 \AA wavelength. The ground state and this first excited state are both doublet states as a result of interaction of the orbital electrons with the nuclear charge in the production of hyperfine splitting. These doublet levels are ninefold and sevenfold degenerate, as will be shown later, and this degeneracy is removed in a magnetic field. As a result of this hyperfine splitting, the 8943.5 \AA "line" actually is made up of four lines, two pairs of which are practically unresolvable; hence, the "line" is seen as two lines 0.3 cm^{-1} (9.192 gc/sec) apart. The electric dipole allowed transitions to make up this line pair number 86 for the 32 energy

levels involved. If circularly polarized light is used in the presence of Zeeman splitting in cesium, this number of 86 allowed absorption possibilities is reduced to 28. If there were very small Doppler broadening in the absorption cell and if the line from the source were considerably broadened, then the transmitted circularly polarized light would appear absorbed at only 22 different frequencies within the band of frequencies of the line pair. The two lines of the 8943.5 Å doublet would be asymmetrically weakened, the higher energy portions being more strongly absorbed. In actual practice, the Zeeman splitting of the levels is small compared with the Doppler broadening so that absorption actually occurs over the band of frequencies appearing in the incident radiation.

Examples of possible absorption in cesium are shown in the energy level diagram of Figure 6. Here are depicted the four levels in question, two each for the cesium ground state and the first excited state. The Zeeman split levels with appropriate m_F magnetic quantum number designations are shown by closely spaced lines. Thus in the $^2S_{1/2}$ levels, the $F = 4$ state splits into 9 sublevels, while the $F = 3$ splits into 7 sublevels. The same splitting numerically occurs for the $^2P_{1/2}$ level, but the energy separation of the sublevels is different in each case, as is shown at the right in $\text{cm}^{-1} \times 10^{-5}/\text{gauss}$ magnetic field strength.

Ordinary selection rules for absorption (and emission) in the $^2S_{1/2} - ^2P_{1/2}$ transition are: $\Delta F = \pm 1, 0$; $\Delta m_F = \pm 1, 0$. In the case of circular polarization, the Δm_F selection rule is modified to either +1 or -1, right or left circular polarization, σ^+, σ^- transitions. Suppose we have the σ^+ case with $\Delta m_F = +1$ and consider the example in the figure. At room temperature the ground state sublevels are all about equally populated. Suppose an atom in the $F=3$ level, $m_F = 2$, absorbs a photon. It can be excited to either the $F = 3$ or $F = 4$ level of the $^2P_{1/2}$ state, but it must have $m_F = +1$ in either case. Upon being excited, the atom immediately releases its newfound energy by spontaneous radiation (in about 10^{-8} sec) and can do so by the ordinary selection rules. This process is shown as (1) in the figure. Assuming that the relaxed atom winds up in the $F = 4$, $m_F = 0$ state, we carry on the process again (2) to $F = 4$, $m_F = +2$ and thence (3) to $F = 4$, $m_F = +4$ of the ground state. It can be seen that no matter what level one starts with initially, it will always be possible to trace the atom by sufficient absorption and reradiations to the $m_F = +4$ state of the $F = 4$ level of the ground state. This is necessary because there is no absorption process allowed in this set of transitions which makes it possible for an atom in this sublevel to be removed from the level. Theoretically, therefore, we see that it is possible to drive all of the absorbing atoms into the $m_F = +4$ sublevel where they can no longer absorb energy unless released by an external mechanism. Therefore, it is clear that transmission of radiation through an absorption cell with optical

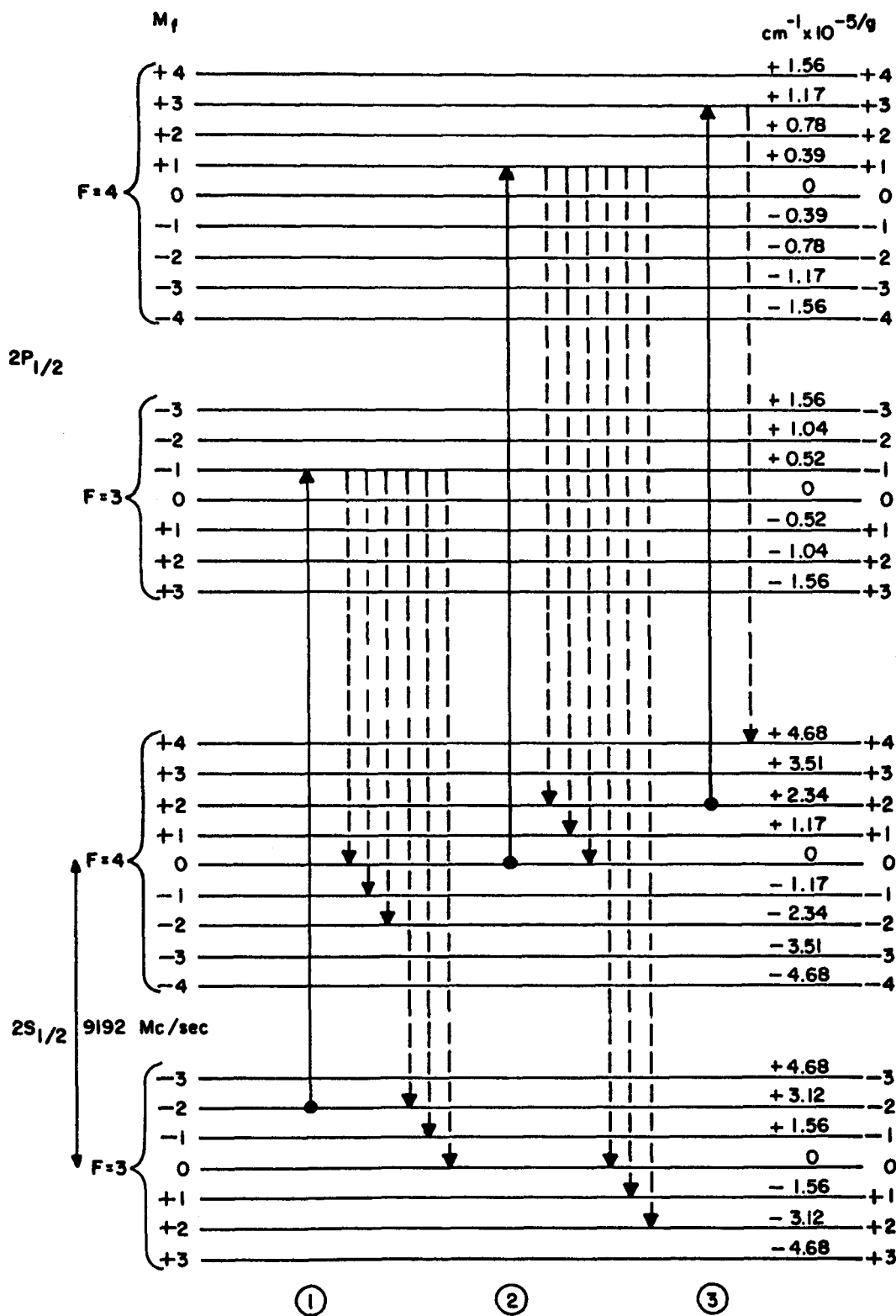


Figure 6. Examples of σ + Absorption and Nonselective Emission in Cesium to Show Optical Pumping

pumping increases with time from switch-on as the inverted population increases, the effect being more pronounced the longer we are able to make the relaxation time of this quasi-metastable state.

A host of studies has appeared in the literature on the effects of buffer gases in the absorption bulb on the relaxation of various species of optically pumped atoms, and a very recent one⁹ provides some useful information on cesium. Different noble gases show different spin disorientation effects for optically pumped atoms, and a mixture of gases at a particular temperature can provide a wide range of relaxation times. A linear relationship, which shows relaxation time decreasing as temperature is increased, is shown in the latest reference. The slope at 50°C is 2.7 milliseconds/degree C for neon buffering for relaxation times as long as 350 milliseconds. The importance of relaxation time in MIROS cross modulation experiments was shown in equation (9).

The level structure depicted in the preceding figure gives an indication of the ways in which two beams of radiation incident on an absorption cell can be made to produce cross-modulation. One beam circularly polarized and monochromatic at the 8943.5 Å wavelength brings about optical pumping with an abnormal population of atoms in the $m_F = +4$ level of the ground state. A second beam of the same wavelength propagated in the same direction could destroy this overpopulation if the state of polarization is different, because a different set of selection rules on Δm_F change would hold. The state of polarization of the second beam can be the linear (plane) type, unpolarized (all types) or circular polarization of the opposite sense of rotation of the electric vector. Any other wavelength light would also be acceptable, as long as absorption from the overpopulated sublevel of the ground state could be effected by such photons. Examples of such transitions are from the ground state $6s^2P_{1/2}$ to $6p^2P_{3/2}$ at 8521.7; to $7p^2P_{1/2, 3/2}$ at 4593.8 and 4555.3; to $8p^2P_{1/2, 3/2}$ at 3888.7 and 3876.4, numbers in Angstrom units, all such lines being of the so-called principal doublet series. The restriction on direction of propagation of the pumping beam is that it be along the magnetic field in order that our $\Delta m_F = +1$ selection rule hold. Clearly, this restriction does not limit direction of propagation of the second beam, since the effect of its photons is to destroy orientation of the pumped atoms with respect to the magnetic field.

9. Franz, F. A. and Luscher, E., "Spin Relaxation of Optically Cesium," Phys. Rev. 135, A582, 1964.

The action of a second beam of radiation is to cause absorption of atoms in the $m_F = +4$ level to an excited state from which spontaneous emission of radiation will cause populations in other magnetic sublevels of the ground state. The diagram of energy levels shows also that the same effect may be brought about by photons of the correct energy to cause transitions within levels of the ground state. This other possibility can be fulfilled in two ways: (1) through transitions between adjacent levels of the Zeeman pattern, as between $m_F = +4$ to $m_F = +3$ of the $F = 4$ level, occurring for energies in the radiofrequency range, and (2) between levels of the hyperfine split pattern, bearing in mind that $\Delta m_F = \pm 1, 0$, as, for instance, between $m_F = +4$, $F = 4$ to $m_F = +3$, $F = 3$, corresponding to microwave frequencies.

Another way that populations of the pumped level may be altered is in modulation of the magnetic field. Pumping is defined for a given direction of magnetic field, either along or opposite to direction of light propagation, thereby prescribing the $+1$ or -1 selection rule for Δm_F and overpopulating either the $m_F = +4$ or $m_F = -4$ level. Magnitude of magnetic field is unimportant unless transitions between Zeeman levels is brought about with the radiofrequency or microwave energies. It is seen that an alternation of direction of magnetic field first along and then opposite to direction of light propagation will result in overpopulating of first the $+4$ and then the -4 sublevel and hence show variations in transmitted light at the frequency of alternation of the magnetic field. Since only small fields are required, the second light beam of arbitrary wavelength can be made to actuate a photon device (solar cell) which can provide alternating current for operation electromagnetic.

Work at this laboratory has been concerned in part with an experimental investigation of the cross modulation capabilities of the optical pumping technique using cesium vapor at room temperature. The four modulation methods have been quantitatively catalogued for our particular absorption bulbs, and representative data are shown in Figures 7, 8, 9, and 10, all for constant pumping beam intensity with cross modulation detected by tuned amplifier measurement of the ac component appearing in the transmitted pumping beam. Figure 7 shows examples of frequency response for a variable applied dc magnetic field; Figure 8 shows the frequency response for a chopped cross beam of cesium light incident on the absorption bulb; Figure 9 shows several response curves for the radio frequency Zeeman resonance cross modulation method; and Figure 10 shows the type of response recorded for the hyperfine resonance transitions in the microwave region of the spectrum. In the latter two cases it was necessary to create a varying magnetic field at right angles to the dc field, and this was done for RF by means of a set of coils and for microwave by beaming the energy from a horn antenna, "Antenna, H" in Figure 5."

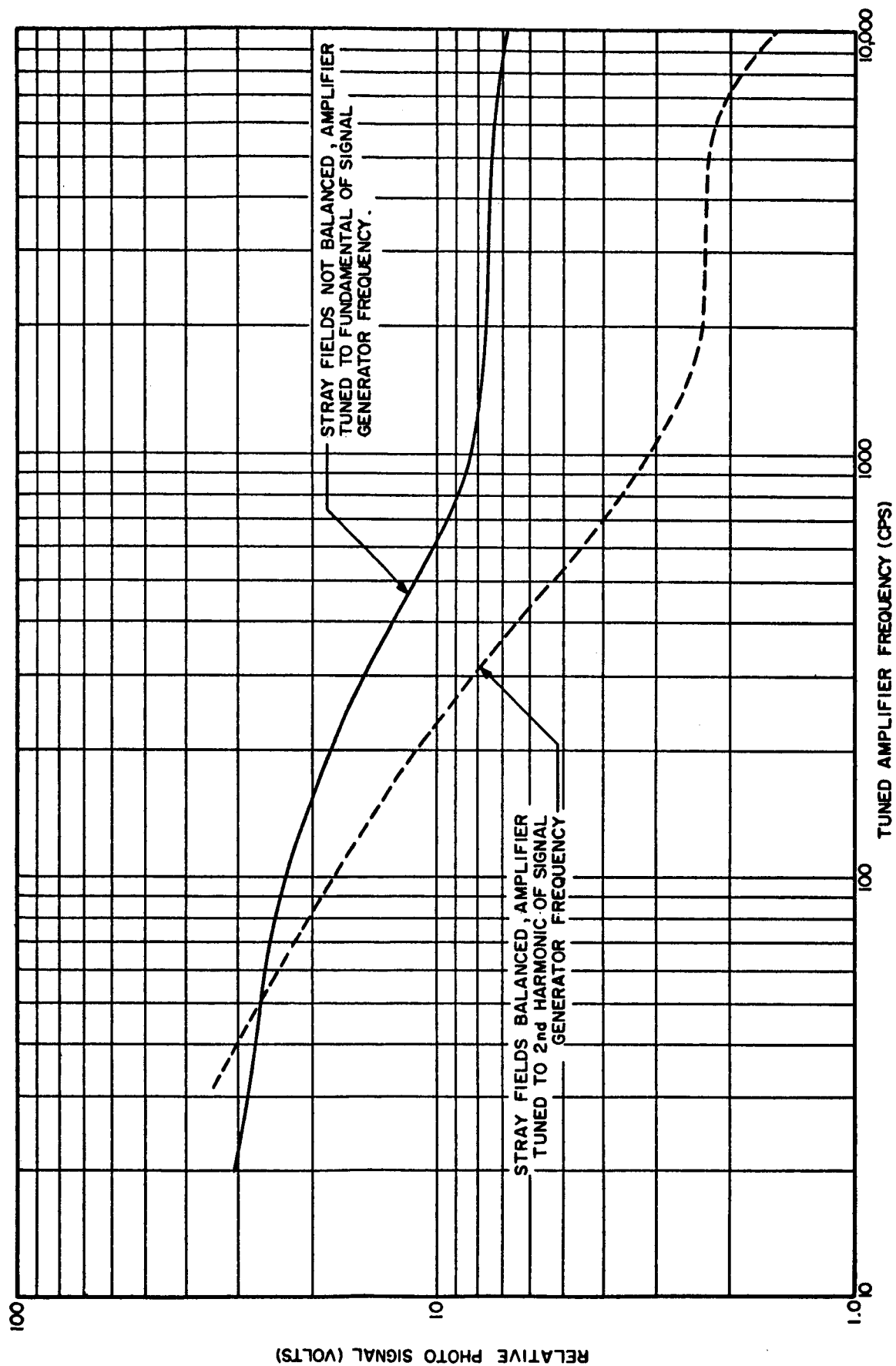


Figure 7 Cross Modulation by Varying Applied Magnetic Field Direction
Variation of Signal as Frequency is Increased Maintaining Constant
Coil Current

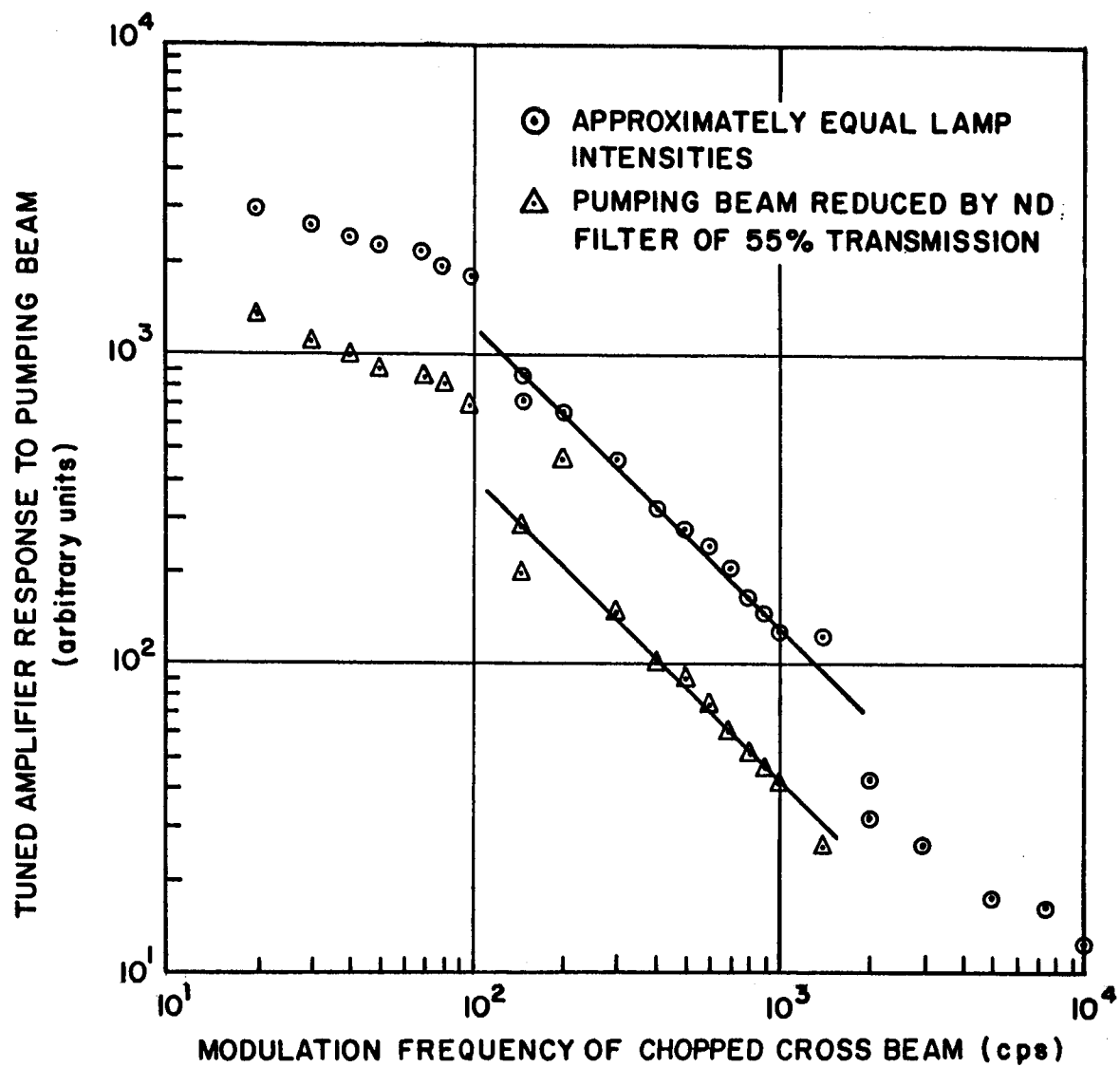


Figure 8. Frequency Response in Optical Cross Modulation

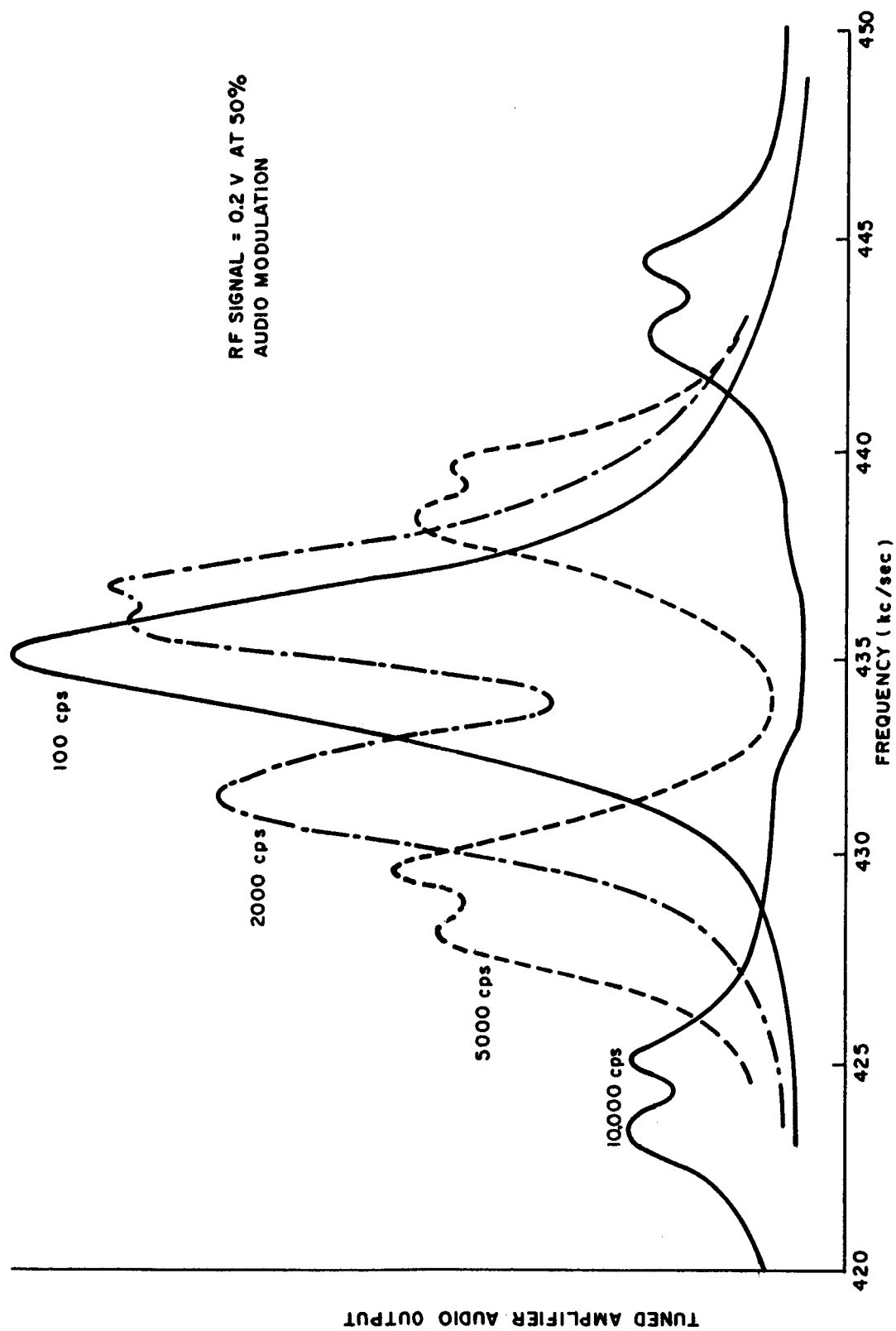


Figure 9. Radio Frequency Case; Response of Optical Pumping System to Audio Modulated Zeeman Resonance Signal for Varying Carrier Frequencies

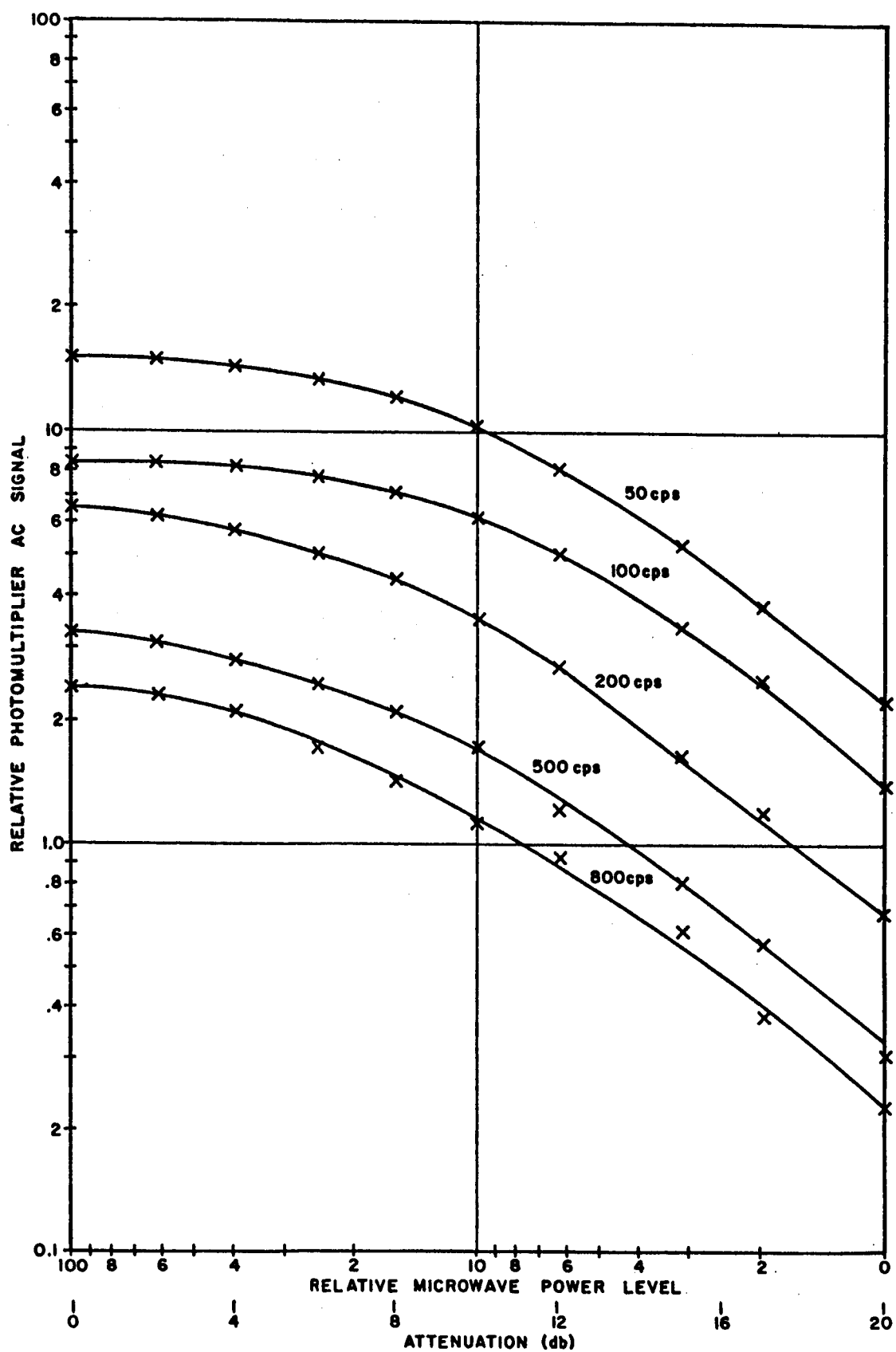


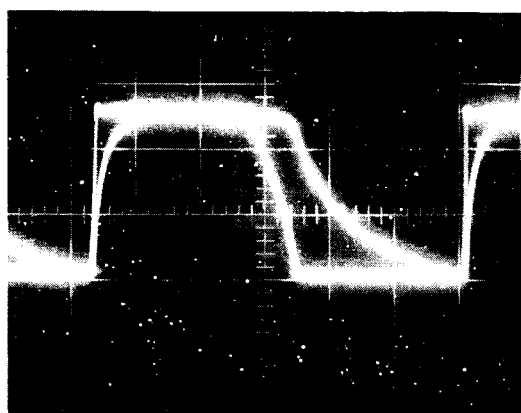
Figure 10. Microwave Case; Cesium Microwave Resonance, Frequency Response to Amplitude Modulation at Audio Ratios - 100 Percent Modulation Level (1000-ml Cell)

Figure 11 shows a set of oscilloscope traces of photomultiplier signals of a transmitted pumping beam and an electronically modulated depumping beam. Where the depumping beam shows sharply varying signals, the pumping beam appears more slowly varying, as a result of the relaxation times associated with the metastable level of the pumped atoms. Two rates are indicated, a fast one for depumping, and a more gradual one for pumping and these two effects become more noticeable as we increase the modulation frequency from 20 to 180 cycles per second.

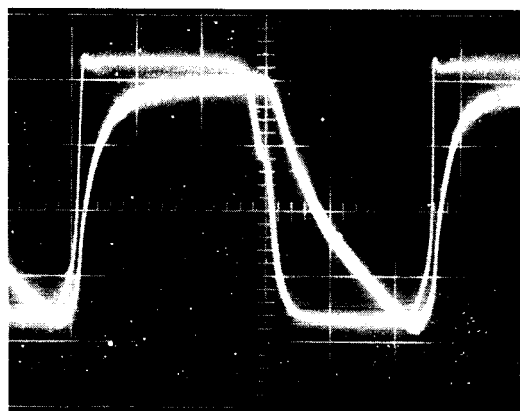
For cross modulation making use of Zeeman resonance frequencies, either for the microwave or the radiofrequency portion of the spectrum, one finds that the resonance bandwidth is very narrow in uniform magnetic fields, as shown in Figure 12, and that the response tends to broaden out as depumping power is increased, thus showing a saturation effect. At a very large power of the depumping beam, the four traces at the top of this figure show marked decrease of signal at the resonance frequency and buildup of the wings of this frequency scan. The curves of this figure are displaced vertically, those marked $G = 0.5$ indicating that they were taken at the same amplifier gain setting at one half the sensitivity as for $G = 1$. The same line-width and saturation indicated in Figure 12 for the radiofrequency case are present for the microwave case of Figures 10 and 13.

Figure 13 is an example of the response obtained when a microwave signal is beamed at an assemblage of pumped atoms for the case of a frequency sweep through the resonance frequency. As in previous cases, several modulation frequencies and power levels are represented.

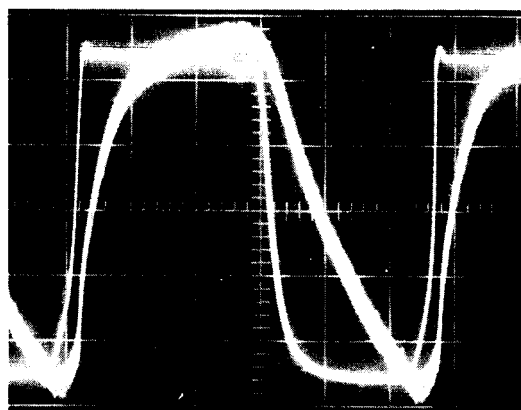
The data in these figures show the responses obtained in the laboratory for one range of pumping intensities, generally $1-100 \mu\text{watts/cm}^2$. It is evident that other responses are available with different pumping intensities, as is clear from the simple theory of Equation 9. For complex signals involving a range of frequencies, it is clear that some compensation in amplification is needed at the output, in order that the received signal at high frequencies be at the same level as for the low frequencies. An interesting example of this need was demonstrated in the construction of a novel standard radio broadcast detector using optical pumping. An antenna on the roof of the laboratory provided a number of local radio station signals which were amplified either 20 or 40 db by a broadband amplifier and fed to a coil around the absorption bulb. The modulation of these signals could be detected if the applied dc magnetic field were tuned to the correct value by a variation of current in Helmholtz coils at the bulb. For low (20 db) signal amplitudes, fidelity was poor, but for large (40 db) signal amplitudes, good reception was the case. The broadening of response indicated in Figure 12



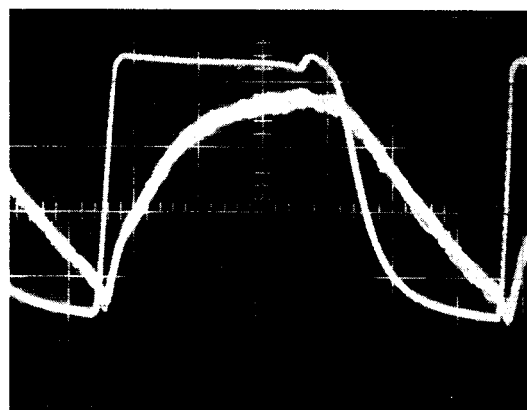
20 cps
10 msec/cm



40 cps
5 msec/cm



80 cps
2.5 msec/cm



180 cps
1 msec/cm

Figure 11. Traces Showing AC Signals of Optical Pumping Beam and Electronically Modulated Cross Light Beam (DC) Signal

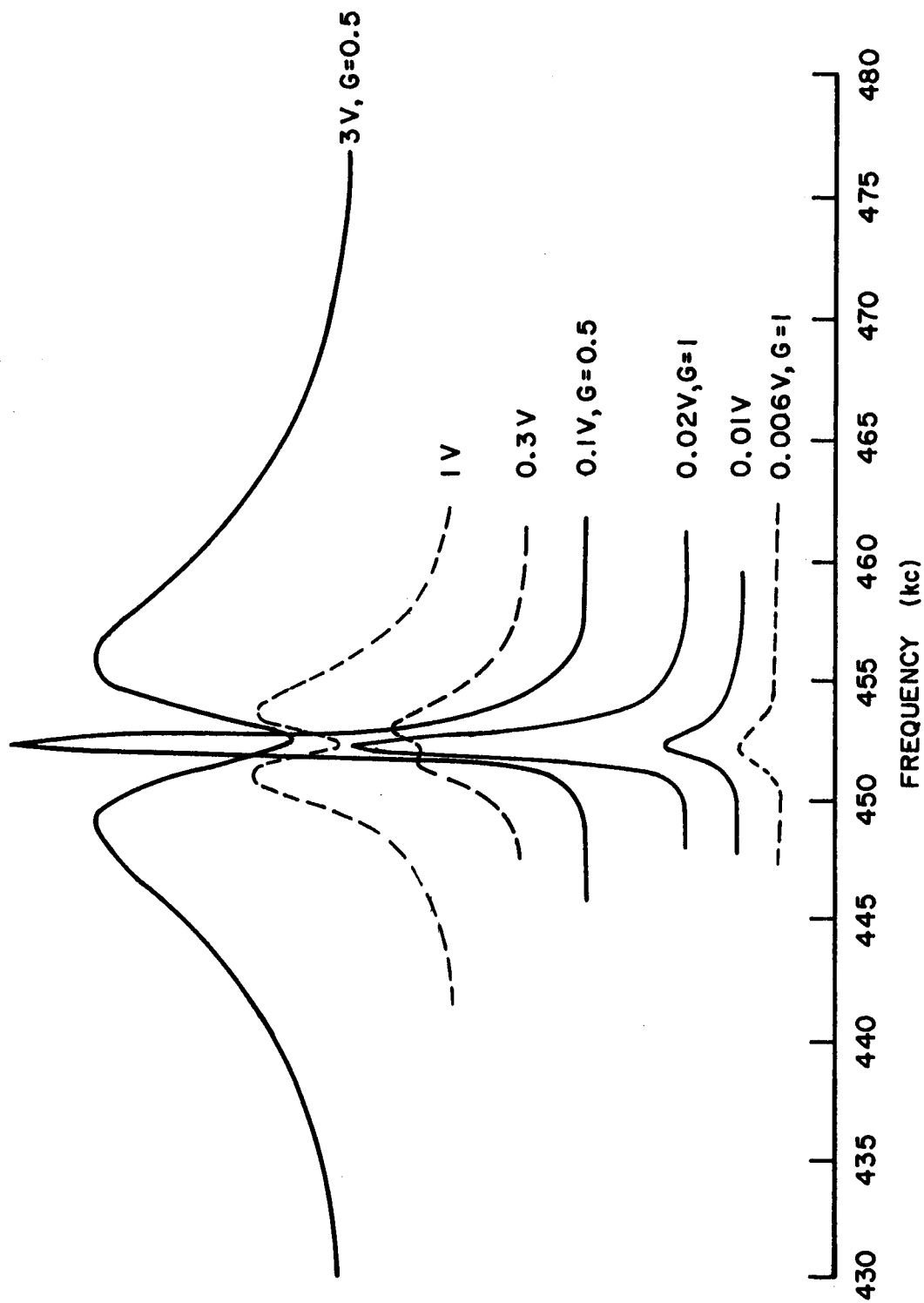


Figure 12. Optical Pumping Transmitted Signal with RF-Zeeman Resonance Radiation; 43% Amplitude Modulated at 100 cps. Signal Generator Voltage and Audio Amplifier Gain are Indicated.

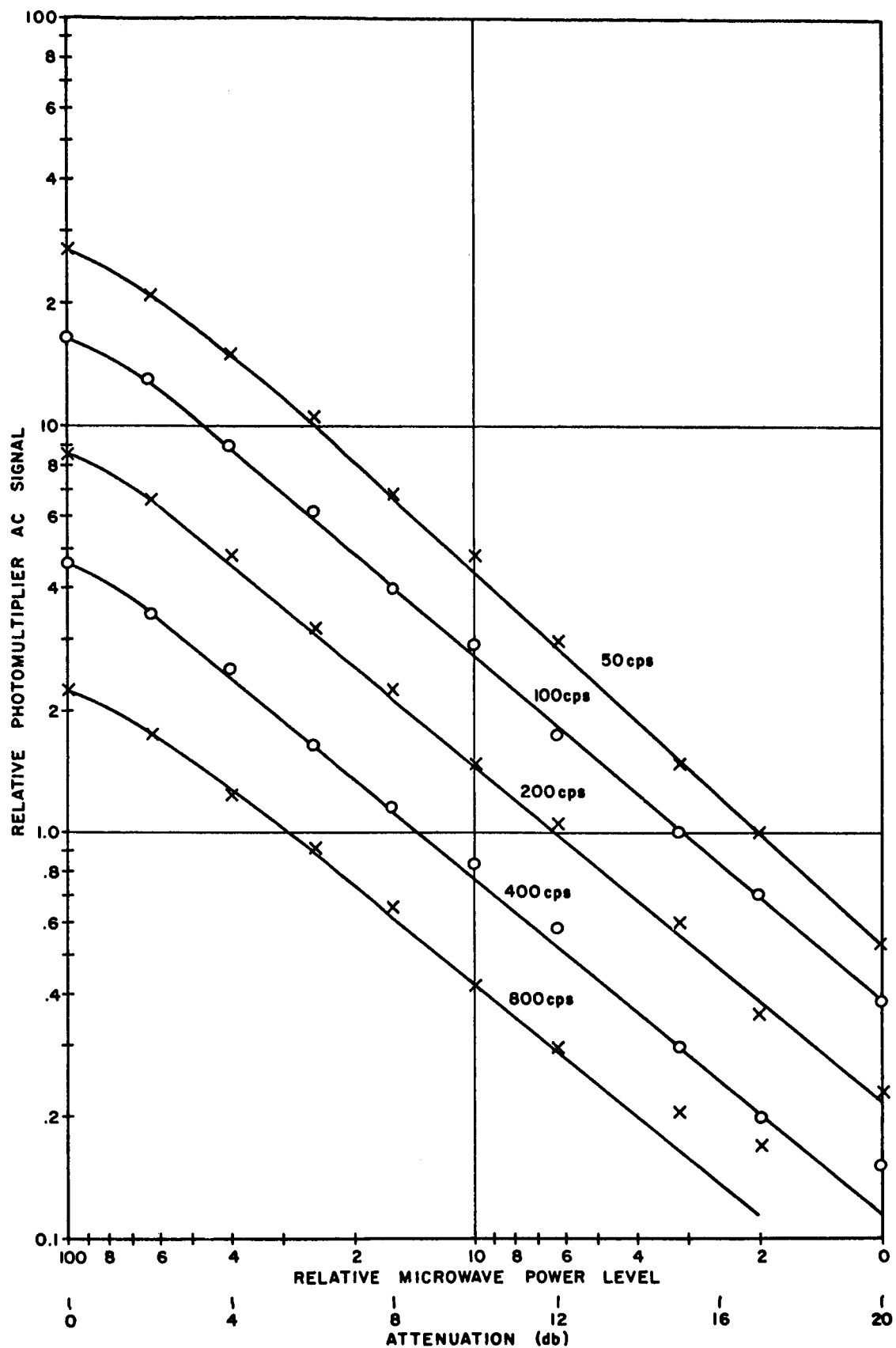


Figure 13. Cesium Microwave Resonance, Response to Frequency Sweep at Audio Rates (1000-ml Cell)

makes it clear that the higher audio frequencies were bolstered as the lower ones decreased in the saturation effect, the proportions of these changes being in the correct ratio for satisfactory fidelity.

3.5.2 Technique of Band Edge Shift

The fact that the application of an electric field across a semiconductor appears to alter the energy separation of the valence and conduction bands associated with intrinsic photoconduction makes the process appear attractive for MIROS cross modulation uses. This intrinsic absorption in some materials is sharply defined in terms of photon energy, appearing in a plot of absorption versus wavelength as an abrupt change (absorption edge) from a small value to a large value of absorption over a small wavelength interval. This edge may be shifted to longer wavelengths with the application of an electric field in a phenomenon known as the Franz-Keldysh Effect. Figure 14 is an attempt to show how electrons associated with these two bands may be considered to participate in the phenomenon. In the presence of an electric field, the energy gap is represented by sloping lines, where it is understood that the vertical separation of the lines corresponds to the photon energy necessary to create a hole-electron pair in excitation of a bound electron to free electron status in the conduction band. With the field, there is increased probability of tunneling through the forbidden region into the conduction band. An electron at point 1 on the figure could move through the gap to point 2 at the same energy but is prevented by the potential barrier 1-1a-2. However, because of the applied field there may be considered to be a finite electron density at the point 3, so that an optical absorption raising an electron to the conduction band may occur at a smaller $h\nu$, equivalent to shifting the band edge to longer wavelengths.

As mentioned previously, this effect can be utilized passively in MIROS with its two beams of radiation in either a two component or a single component device. The first of these would obtain the necessary electric field to apply across the absorption material in question from a separate photovoltaic cell energized by one of the beams; in such a device the second beam would be absorbed in proportion to the electric field obtainable in this manner. The second device accounts for both processes to occur within a single package, the point being to construct a p-n junction device which has a built-in electric field due to charge diffusion. Suppose the n-type material absorbs a short wavelength radiation which causes hole-electron pairs; then, the built-in field will be altered in proportion to the additional charge due to this absorption and will therefore cause a shift in the absorption characteristics of the p-n material. Of course, it is clear that junction width and concentrations of the n- and p-type materials must be chosen with care.

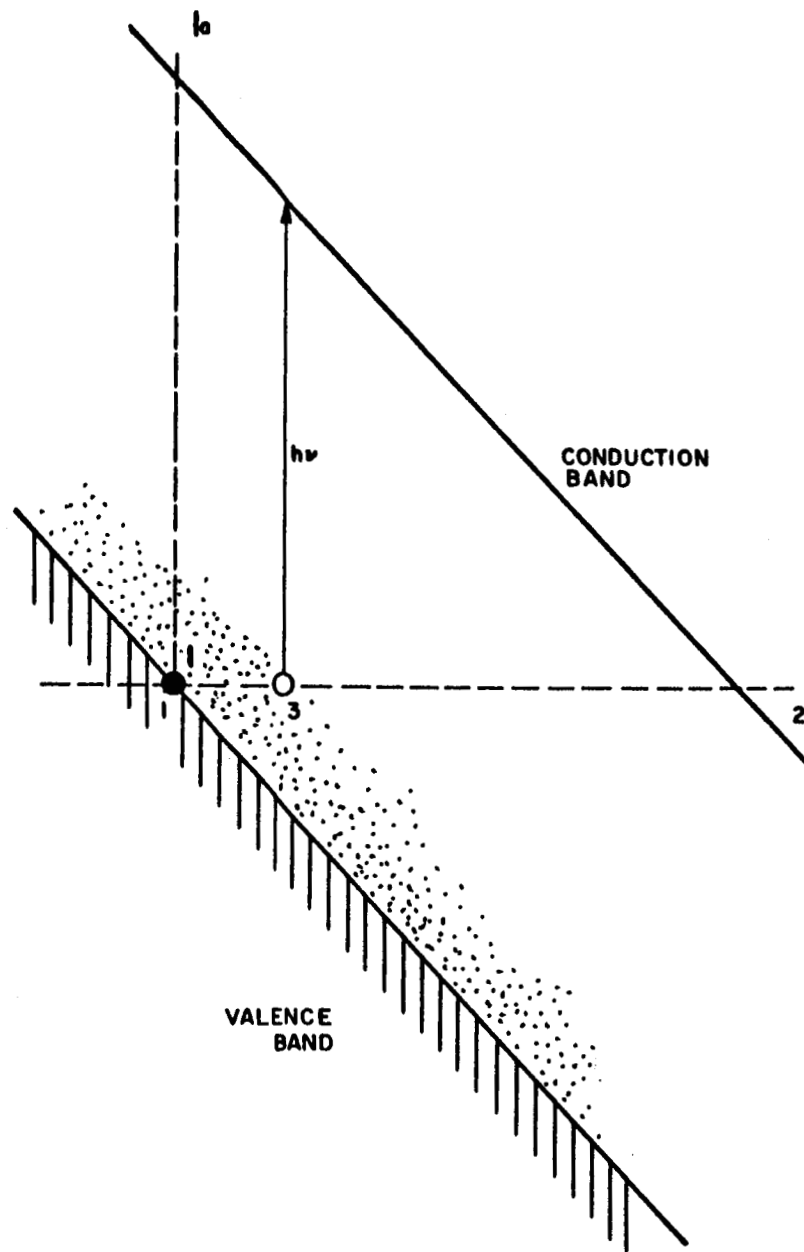


Figure 14. Energy Diagram to Show Tunneling Mechanism with Applied Electric Field

An experimental program was undertaken to investigate the action of such a p-n junction in gallium arsenide (GaAs). The Burstein shift for this material causes the p-region to absorb radiation at longer wavelengths than is absorbed in the n-region, and, consequently, the absorption edge for p-type occurs at lower energies than the n-type. Light of the proper wavelength to be absorbed at the p-type absorption edge will pass through an n-region practically completely without absorption. The p-region is therefore chosen to accommodate the modulating field and is less heavily doped than the n-region; the latter is deliberately heavily doped to bring about as large a Burstein shift to higher energies (filling up of lower energy states) of absorption as possible. Since partial absorption only is desirable in MIROS work, it is necessary to keep the absorbing layers very thin.

Experimental difficulties in this work included the development of a technique to obtain the correct dopings and to reduce the samples to extremely thin dimensions. First efforts were aimed at obtaining lightly diffused p-regions in n-type materials, but later success at electrolytic jet etching allowed the possibility of diffusion of n-type impurities into p-type bases. This etching technique was developed so that reproducibility was assured, and made it possible to design elements consisting of heavily doped n-regions on lightly doped p-type bases. Tin was diffused into GaAs of approximately 5×10^{16} p-type carriers/cc. The diffusion occurs in a thin layer near the surface, and in order to produce thin p-layers on the n-layers, the p-material is etched away from the reverse side, as shown in Figure 15.

Two methods were used to determine the field-induced change in absorption of GaAs samples such as shown in the sketch. Both methods involved the application of a field using an external circuit, rather than the more desirable dual light beam and open circuit operation of the p-n junction, as suggested for MIROS adaptation. One of these techniques involves measuring sample transmission at zero bias and comparing this measurement with that for a dc reverse bias; the light is interrupted by a mechanical chopper so that ac components may be detected. The second technique eliminates the chopper by varying junction voltage around a fixed dc bias; transmission of light from a constant intensity source is modified at the frequency of junction voltage variation. Results obtained by the two methods agree, and a summary of typical results is shown in Figure 16.

The slope of the curve of absorption (α) vs wavelength λ ; i. e., $d\alpha/d\lambda$, will show a maximum at the wavelength of interest in MIROS work. In Figure 16 such a curve is indicated by the solid line for a GaAs sample. The peak amplitude variation of the transmitted light occurs at a shorter

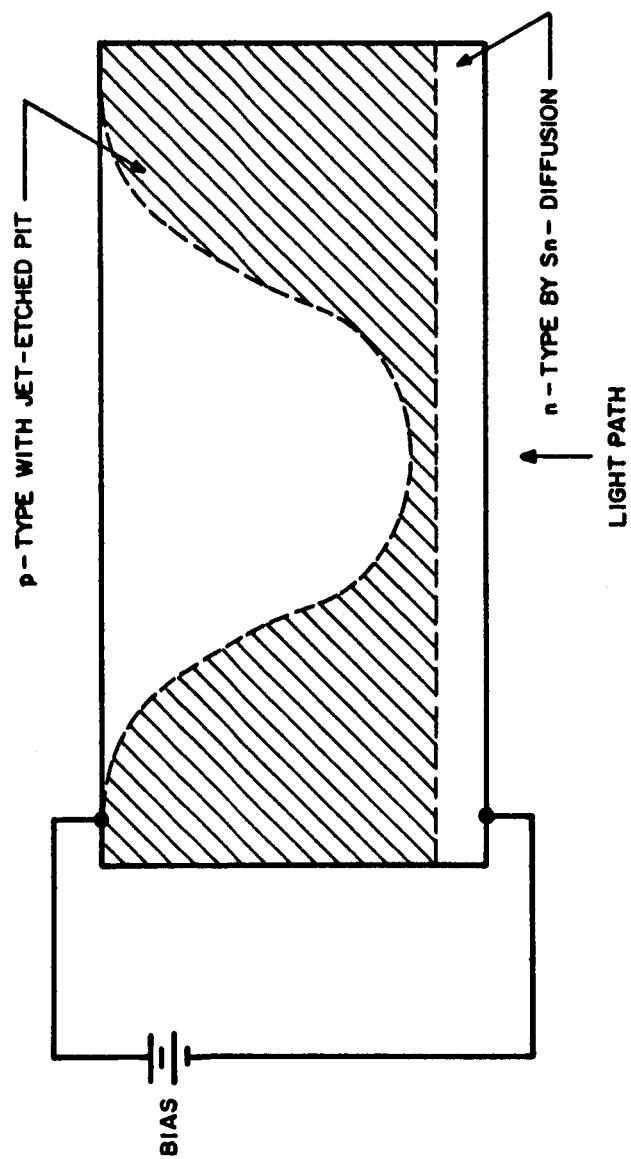


Figure 15. Sketch of Band Edge Modulator Fabricated at Philco

SAMPLE Sn 6 - 2

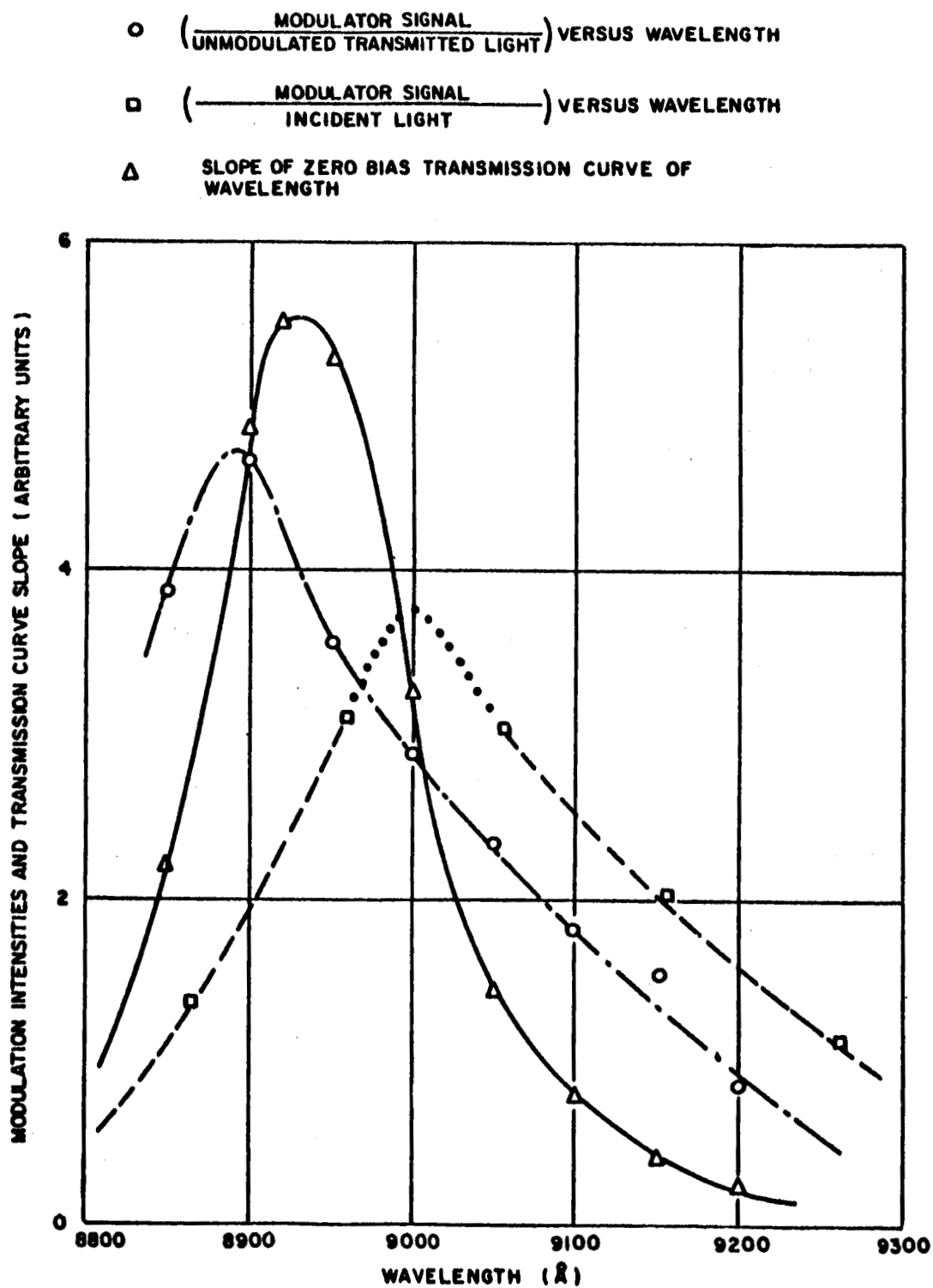


Figure 16. GaAs Edge Effect Modulator

wavelength than one might expect from the maximum of this slope curve. Some experimental error is probably involved in this measurement because of the decrease of transmitted light (greater absorption) as λ is decreased. Figure 16 also shows a curve of ratio of intensity of transmitted light to incident light with a maximum at a wavelength longer than λ_{max} of the slope curve. Such an apparent shift is possibly explained by the fact that larger transmissions at longer wavelengths tend to mislead with larger modulation signals in spite of the fact that the percentage of modulation of the transmitted light may be smaller than for shorter λ 's. Thus, accurate measurements are difficult on either side of the maximum of the slope curve because of low transmission on the one side and high transmission on the other.

Figure 16 indicates modulations of about 5% of incident light available with this particular sample of GaAs. A maximum modulation index can be calculated making use of published data and appears to be about 8%. Other materials may be used for this band edge shifting technique, indium phosphide, for instance, appearing to be roughly twice as good as GaAs with the associated wavelength of transmission at about 1 micron. The frequency response measured for the jet etched GaAs samples was fairly good, the signal at 100 kc/sec being about 3 db down from that of 1 kc/sec, and observations indicate that the edge effect modulator is usable at frequencies beyond 1Mc/sec. Part of this response falloff is due to the geometry (electrode effects), and the results are not to be considered as maximum.

The band edge modulators made with the electrolytic jet etch method of fabrication were very small in area (20 - 40 mils diameter) and difficult to use for quantitative measurements. Larger area junctions can be produced by etching, but it is more advisable to develop an epitaxial growth technique for uniformity of layer thickness and ease in handling the finished product. MIROS requirements on area of the devices depend, as mentioned previously in this report, on whether or not light collection is performed at the satellite.

4. CONCLUSIONS AND RECOMMENDATIONS

We have presented a list of proposed MIROS mechanisms, discussions on MIROS requirements and information on experimental activities concerning two of the proposed mechanisms. It seems appropriate in this final section to compare briefly the various schemes in the formulation of recommendations for further work in MIROS development program.

Two different techniques were demonstrated as capable of intelligibly transferring modulation from one light beam to another in a passive manner

without the use of external power equipment. From this work and related analytic activities, several generally pertinent facts have evolved:

1. Optical communication by this means is definitely possible and depends only on the successful adaptation of light sources, primarily in intensity and in some cases wavelength, to the absorption bands of the MIROS element. Very long distance communications require coherent sources of very high power and low beam divergence, preferably with wavelengths in the red or infrared portions of the spectrum to match atmospheric "windows" and avoid large scale absorptions and small particle scattering losses. Wavelength matching of laser sources is entirely feasible at this time by proper concentrations of components in injection lasers, and a number of distinctive atomic absorptions are accessible with such sources.

2. Continuous sources are particularly desirable for wideband communications. While the present day pulsed laser sources of higher power are applicable for MIROS needs in long distance propagations, the extent of information that can be transmitted is limited because of low repetition rates. Long distance and wideband transmission specifications demand that the desirable power ranges of our (CW) laser sources lie in the 1 - 50 watt class for low altitude satellites and above 1 kilowatt for the synchronous satellite, all of which need yet to be developed.

3. Absorption coefficients for MIROS elements must be high, and relaxation times must be chosen to be compatible with the desired wideband responses. An analysis of rate equations pertaining to equilibrium populations of metastable states in MIROS two-photon processes shows that an inevitable ω^{-1} falloff in response occurs which can be delayed in the modulation frequency spectrum by a suitable choice of the intensities of the MIROS optical beams. Narrow-band atomic ground-to-excited state resonance absorptions appear to be useful, because oscillator strengths are usually high and filtering needs in the presence of stray radiations are not as great as with other processes.

The question of sensitivity led this research group to eliminate several MIROS mechanisms from serious consideration. A literature survey showed that the oscillator strengths for absorptions of rare earth ions in lattices were less than 10^{-3} and as bad as 10^{-6} - 10^{-7} . While these are not bad enough to prevent laser action when the lattices are "pumped" by very intense sources, they are not good enough to allow cross modulations with microwatt intensities. Molecular species generally show very low oscillator strengths for their rotation-vibration transitions, and for the same reason, no specific molecular process was sought for detailed treatment. Photochromic materials

were not investigated in quantitative analysis for two reasons: (a) the amount of information at present is very scarce and (b) available information leads us to believe that changes in transmission are most noticeable in the range of high incident intensities where other processes are much more attractive. Free carrier absorptions were eliminated, in spite of efficient absorptions of the free carriers, because of difficulty of first producing the carriers by a light beam. Of those processes mentioned earlier in the report as possibly being useful, from an intensity point of view, only those remaining are the band edge shift, optical pumping of alkali metal vapors and the F - F' center conversion in alkali halide crystals.

The conversion of F-centers to F'-centers is reported to be a very efficient process which takes place over fairly wide spectrum bands. As a MIROS contender it would require narrow-band filtering in order to restrict absorptions to the laser wavelengths used, but its wideband nature does make several existing lasers useful, including the high powered ruby. However, we show in Equation 3 that the absorption of monochromatic radiation at any given wavelength decreases as the line width increases. Also, as a solid state device depending on the mobility of freed carriers from one trapping site to another, the F-center MIROS element would be quite temperature sensitive, operating most efficiently at a low temperature but restricted to low modulation frequencies because of low mobilities. Superposition of MIROS beams is required, because diffusion lengths of carriers could not be expected to exceed a few microns.

Similar solid state considerations apply in the case of the band edge shifting technique. Narrow-band filtering is required here also, but not quite as stringently, since only the high energy beam in this technique determines the shifting of the band edge. In wavelength, somewhat less latitude is allowed with band edge shifting, since one of the wavelengths must be chosen to match the position of the edge. The high energy beam can have any wavelength which lies in the intrinsic absorption region of the n-type material, as described for the Philco device. It will be recalled that the 5% modulation reported for this scheme was measured at room temperature. Other temperatures of operation are available. The position of the edge moves to shorter wavelengths as temperature is lowered. Moss¹⁰ reports that this shift frequently amounts to about 4×10^{-4} eV/°C, or about $3.23 \text{ cm}^{-1}/^\circ\text{C}$, corresponding to about 3 Å/degree C shift at 1μ wavelength. This large variation is probably more than desirable with most lasers, but it is useful

10. T. S. Moss, "Optical Properties of Semi-conductors," Butterworths Scientific Publications, London, 1959, p. 45.

so far as tunability is concerned. It is clear that carrier mobility should be no better for band edge shifting than for color center conversion for MIROS applications. The possibility of using band edge shift in a separate device from that which is used to create the electric field (separate photovoltaic cells) makes this somewhat more versatile in an optical communications link than the color center scheme.

Optical pumping of alkali metal vapors in our estimation appears to be one of the best techniques for application to the passive needs of a MIROS system. This scheme offers high sensitivity, narrow absorptions, good carrier diffusion and relative ease in developing and constructing. Several disadvantages are apparent, none of which are insuperable. The wavelengths for pumping and depumping are critical and require careful tuning of the lasers in order that large percentage changes in transmission may be attained. There is a fairly large temperature sensitivity in the absorption coefficient, as a result of large vapor pressure changes which result in varying number densities; these changes can be offset by changes in transmitted intensity. The theoretically indicated ω^{-1} falloff in reception of the modulated signal was approached at audio frequencies in laboratory experiments on optical pumping. Higher light beam intensities are needed to expand bandwidth well beyond the audio range. The need of circularly polarized light may introduce some loss of intensity at the source, since this would be obtained ordinarily through use of a retardation filter in conjunction with a linearly polarized laser. Long distance atmospheric transmission characteristics of circularly polarized coherent light have never been measured, as far as this research group is aware, but no special losses are expected. There are several choices of materials in optical pumping, all of them alkali metals. Helium and mercury could be used, but not in a passive system. Cesium was chosen for laboratory investigation because of its applicability at room temperature. At a satellite where any desired ambient temperature over that of "dark" space is attainable by proper choice of design and materials, the higher temperatures required for rubidium, sodium or potassium may also be reached. There is a possibility that rubidium is slightly more efficient in its correct operational range (60°C) than cesium in its range, because of its lower nuclear spin and fewer allowed transitions in pumping. Experimental data on relative efficiencies are not available on this point.

Conclusions developed herein on power level required for transmission have not accounted for absorptive, refractive and scattering losses in the atmosphere. The percentage loss probably changes from day to day and season to season as atmospheric conditions change. Without stipulating the wavelength of transmission and atmospheric transmission parameters, one

finds it difficult to arrive at correct attenuation factors which are known to vary over several orders of magnitude from the extreme conditions of unlimited visibility to very dense fog.

Recommendations of the Philco research group as a result of this analytical and experimental program are as follows:

a. Develop a passive MIROS system for a low altitude satellite of not more than 500 miles so that lasers of 1 - 10 watts power and readily attainable beam angle may be considered for CW transmission. The objective of the 22,000 mile synchronous satellite requires very high power lasers, which would probably be pulsed at repetition rates too low to be capable of transferring large bandwidth intelligence.

b. Consider for development the modulation inducing scheme of optical pumping of one of the alkali metal vapors. Absorption cells containing the material and a buffer gas would be used in conjunction with corner cube retrodirective reflectors.

c. Consider for development the tunable type laser for matching the wavelength of the modulation inducing scheme, GaAs-P for rubidium, GaAs-InAs for cesium, for instance. At present CW injection lasers of single mode output produce power in the milliwatt range, but it is expected that advancements in technology will rapidly increase these levels.

APPENDIX I

SUPPLEMENTARY BIBLIOGRAPHY

Among the many references to information concerning MIROS mechanisms which were used during the course of this investigation, supplementary to those listed in the body of the report and previously mentioned in the monthly contract progress reports are:

1. OPTICAL PUMPING

- a. Bloom, A. L., "Optical Pumping," Scientific American, Vol. 203, No. 4, October 1960, p. 72.
- b. Hawkins, W. B., "Orientation and Alignment of Sodium Atoms by Means of Polarized Resonance Radiation," Physical Review, 98, 478, 1955.
- c. Franzen, W., "Spin Relaxation of Optically Aligned Rubidium Vapor," Physical Review, 115, 850, 1959.
- d. Dehmelt, H. G., "Slow Spin Relaxation of Optically Polarized Sodium Atoms," Physical Review 105, 1487, 1957.
- e. Dehmelt, H. G., "Modulation of a Light Beam by Precessing Absorbing Atoms," Physical Review 105, 1924, 1957.
- f. Kastler, A., "Displacement of Energy Levels of Atoms by Light," J. Opt. Soc. Am., 53, 902, 1963.
- g. Arditi and Carver, "Frequency Shift of the Zero-Field Hyperfine Splitting of Cs^{133} Produced by Various Buffer Gases," Physical Review, 112, 449, 1958.
- h. Skalinski, T., "Orientation Optique des Atomes dans la Vapeur de Cesium," Le Journal de Physique et Le Radium, 19, 890, 1958.
- i. Franz, F. A., "Cs Lamp for Optical Pumping," Rev. Sci. Instr., 34, 589, 1963.

- j. Bell, W. E., Bloom, A. L., and Lynch, J., "Alkali Metal Vapor Spectral Lamps," Rev. Sci. Instr., 32, 668, 1961.
- k. Kusch, Millman and Rabi, "The Radio Frequency Spectra of Atoms - Hyperfine Structure and Zeeman Effect in the Ground State of Li^6 , Li^7 , K^{39} and K^{41} ," Physical Review, 57, 765, 1940.
- l. Alezandrov, E. B. and Kchodovoj, V. A., "On Dehmelt's Experiment," Proceedings of the 3rd Quantum Electronics Conference, Quantum Electronics III, Columbia Univ. Press, 1964, p. 299.
- m. Lipworth, E., "Proposed Method for the Enhancement of Optical Pumping Double-Resonance Signals," Proceedings of the 2nd International Conference on Quantum Electronics, Advances in Quantum Electronics, Columbia Univ. Press, 1961, p. 293.
- n. Althoff, K., "Hochfrequenzübergänge im angeregten $7^3\text{P}_{3/2}$ Zustand des Cäsiumatoms und Bestimmung des Quadrupolmomentes des Cäsium¹³³ - Kernes," Zeitschrift für Physik, 141, 1955, pp. 33-42.

2. OTHER MIROS MECHANISMS

2.1 Color Centers:

- a. Amelinckx, S., "Radiation Effects in Ionic Crystals," Proceedings of the International School of Physics "Enrico Fermi," Italian Physical Society, Course XVIII, "Radiation Damage in Solids," edited by D. S. Billington, Academic Press, New York, 1962, p. 422.
- b. Pick, H., "Color Centers in Alkali Halides," Suppl. Nuovo Cimento, Vol. 7, 1958, p. 498.

2.2 Band Edge Shift

- a. Franz, W., "Einfluss eines elektrischen Feldes auf eine optische Absorptionskante," Zeits. Naturforschung, 13a, 1958, p. 484.

- b. Keldysh, L., Vavilov, V., and Bricin, K., Proceedings of the International Conference on Semiconductors, Prague, 1960, p. 824.
- c. Braunstein, R., Pankove, J. L., and Nelson, H., "Effect of Doping on the Emission Peak and Absorption Edge of GaAs," Appl. Phys. Letters, 3, 31, 1963.

2.3 Free Carriers

- a. Lasser, M. E., Cholet, P. H. and Emmons, R. B., "Electronic Scanning System for Infrared Imaging," Proc. IRE, 47, 2069, 1959.
- b. Desvignes, F., "Optical Absorption by Free Hole-Electron Pairs Liberated by the Photoelectric Effect in a Germanium Single Crystal," C. R. Acad. Sci. (Paris), Vol. 246, No. 12, 1824-7, March 24, 1958.
- c. Huldt, L., "Determination of Free Carrier Lifetimes in Semiconductors from the Relaxation Time of Photo-excited Infrared Absorption," Arkiv for Fysik, 15, 229-36, 1959; also Ark. Fys. 20, 527, 1962.
- d. McQuistan, R. B., Schultz, J. W., "Modulation of Infrared by Free Carrier Absorption," J. Applied Physics, 35, April 1964, p. 1243.

2.4 Other

- a. Cohen, A. J. and Smith, H. L., Science, 137, 981, 1962, photochromic materials.
- b. Johnson, L. F., "Optical Maser Characteristics of Rare Earth Ions in Crystals," J. Applied Physics, Vol. 34, 1963, p. 897; 2-photon absorption in crystals.
- c. Landolt-Bernstein, Zahlenwerte und Funktionen, Vol. I, "Atom- und-Molekularphysik, Part I, Atome und Ionen," Springer, 1950, p. 260; oscillator strengths of atoms.

APPENDIX II

POWER REDUCTION FACTORS IN LASER TRANSMISSION
FOR VARIOUS DISTANCES (r) AND BEAM DIVERGENCES (θ)
CALCULATED ACCORDING TO $(r\theta)^{-2}$

θ (sec) \ r	100 mi.	1000 mi.	10,000 mi.	22,289 mi.
1	1.64×10^{-2}	1.64×10^{-4}	1.64×10^{-6}	3.3×10^{-7}
5	6.5×10^{-4}	6.5×10^{-6}	6.5×10^{-8}	1.3×10^{-8}
10	1.64×10^{-4}	1.64×10^{-6}	1.64×10^{-8}	3.3×10^{-9}
15	7.2×10^{-5}	7.2×10^{-7}	7.2×10^{-9}	1.3×10^{-9}
20	4.1×10^{-5}	4.1×10^{-7}	4.1×10^{-9}	8.2×10^{-10}
25	2.6×10^{-5}	2.6×10^{-7}	2.6×10^{-9}	5.2×10^{-10}
30	1.8×10^{-5}	1.8×10^{-7}	1.8×10^{-9}	3.7×10^{-10}
60	4.5×10^{-6}	4.5×10^{-8}	4.5×10^{-10}	9.2×10^{-10}

APPENDIX III

EDGE SHIFT DATA

1. EXPONENTIAL EDGE APPROXIMATION

Assume an absorption edge of the form

$$\alpha = \alpha_0 \exp \gamma (E - E_0), \quad (1)$$

where γ is the "steepness factor" defined in $[\text{ev}^{-1}]$. Values of α_0 , γ , and E_0 , as well as the range of validity for this expression, appear in Table I.

TABLE I

Material	$\alpha_0 = \alpha(E_0)$ cm^{-1}	E_0 ev	α ev^{-1}	Range of Validity		$\alpha(E_f)$ cm^{-1}
				E_0	E_f	
GaAs	10	1.36	100	1.36	- 1.42	3×10^3
CdS	10	2.37	100	2.37	- 2.45	2.5×10^4
Se	10	1.7	16	1.7	- 2.2	10^5
InSb(77°K)	1	0.207	460	0.197	- 0.225	10^3
InAs	1	0.308	150	0.308	- 0.360	10^3
InP	1	1.27	140	1.27	- 1.34	10^4

2. FRANZ-KELDYSH SHIFT

The shift of the optical absorption edge $\delta E(\text{ev})$ as a function of applied field F (volts/cm) is given by

$$\frac{\delta E}{F^2} = \frac{\gamma^2 6.4 \times 10^{-17}}{m^*/m_0} \left[\frac{\text{ev}}{(\text{volts/cm})^2} \right], \quad (2)$$

where m^*/m_0 is the effective mass ratio for electrons. Table II contains measured and calculated values of this edge shift factor.

TABLE II

Material	m^*/m_0	$\left(\frac{\delta E}{F^2}\right)$ Calculated ev/(volt/cm) ²	$\left(\frac{\delta E}{F^2}\right)$ Measured ev/(volt/cm) ²
GaAs	0.065	9.8×10^{-12}	8.5×10^{-12}
CdS	1.0	6.4×10^{-13}	2.2×10^{-15}
Se	2.5	6.5×10^{-15}	
InSb(77°K)	0.013	9.2×10^{-10}	
InAs	0.02	7.5×10^{-11}	
InP	0.065	2×10^{-11}	

On the basis of the calculated and experimental values and on the technology for controlling the characteristics of III-V materials, these offer the best possibilities for field effect electro-optical elements.

3. EDGE EFFECT MODULATOR

Consider a P-N junction of the following form:

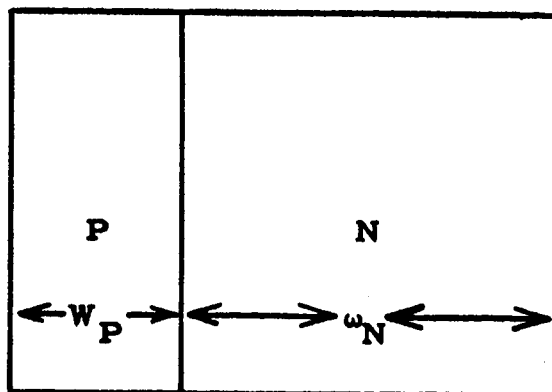


Figure 1

If the doping density of the N region is much higher than the doping density of the P-region, then the diffusion potential, V_J , produces a built-in field, E , in the P-region. The magnitude at this field is given by

$$E \approx \frac{V_d}{X_j} \approx \frac{E_{\text{gap}}}{X_j} \quad (3)$$

X_j , the width of the depletion region, is a function of the junction doping. For III-V compounds with ϵ , the dielectric constant $\sim 12 - 16$ is given in Table III.

TABLE III

Doping Level cm^{-3}	X_j cm	$E(\text{GaAs-InP})$ volts/cm	$E(\text{InAs})$ volts/cm
10^{14}	3×10^{-4}	3×10^3	10^3
10^{15}	10^{-4}	10^4	3×10^4
10^{16}	3×10^{-5}	3×10^4	10^4
10^{17}	10^{-5}	10^5	3×10^4

If light impinges on the P-N junction and if open-circuit operation is considered, then the junction field is greatly reduced. Therefore, the optical absorption in the region X_j decreases in going from a dark to a light condition. For wider gap material with low leakage current (I_0), this requires less optical energy than is required for narrower gap materials; on the basis of this criterion, GaAs and InP would appear promising. Optical absorption in the N-region can be ignored because of the Burstein shift. This device is most efficient when $W_p \sim X_j$; if $W_p > X_j$ then the light transmitted at the band edge in both light-on and light off conditions of the modulating light is attenuated by a factor $e^{-\alpha(W_p - X_j)}$, where α is the absorption constant of P-type material (zero field case) at the wavelength under consideration.

For $W_p \sim X_j$,

$$T_L = I_0 e^{-\alpha X_j}$$

$$T_D = I_0 e^{-\alpha(F)X_j}$$

$$\frac{T_L - T_D}{T_L} = M_F = 1 - e^{-[\alpha(F) - \alpha] X_j}, \quad (4)$$

where $\alpha(F)$ is the absorption constant at the junction field, I_0 is the intensity of the incident light, T_L and T_D are the transmissions in the light and dark, respectively, and M_F is the percent of modulation. Figure 2 contains a plot of T_L , M_F , and $T_L - T_D$ vs X_j in units of $1/\alpha(F)$ for a ratio of $\alpha(f)/\alpha$ equal to 2. Observe that the M_F figure of merit goes to unity as the junction thickness increases; however, the value of T_L goes to zero for this region. Therefore we should use $T_L - T_D$ as a figure of

merit. Figure 3 contains a plot of $\left(\frac{X_j}{\alpha(F)}\right)_{T_L - T_D = \max}$ vs $\frac{\alpha(F)}{\alpha}$, illus-

trating the variation of this max difference point as a function of absorption constant ratio as well as a plot of $(T_L - T_D)_{\max}$ as a function of the

$\left(\frac{X_j}{\alpha(F)}\right)_{T_L - T_D = \max}$ value.

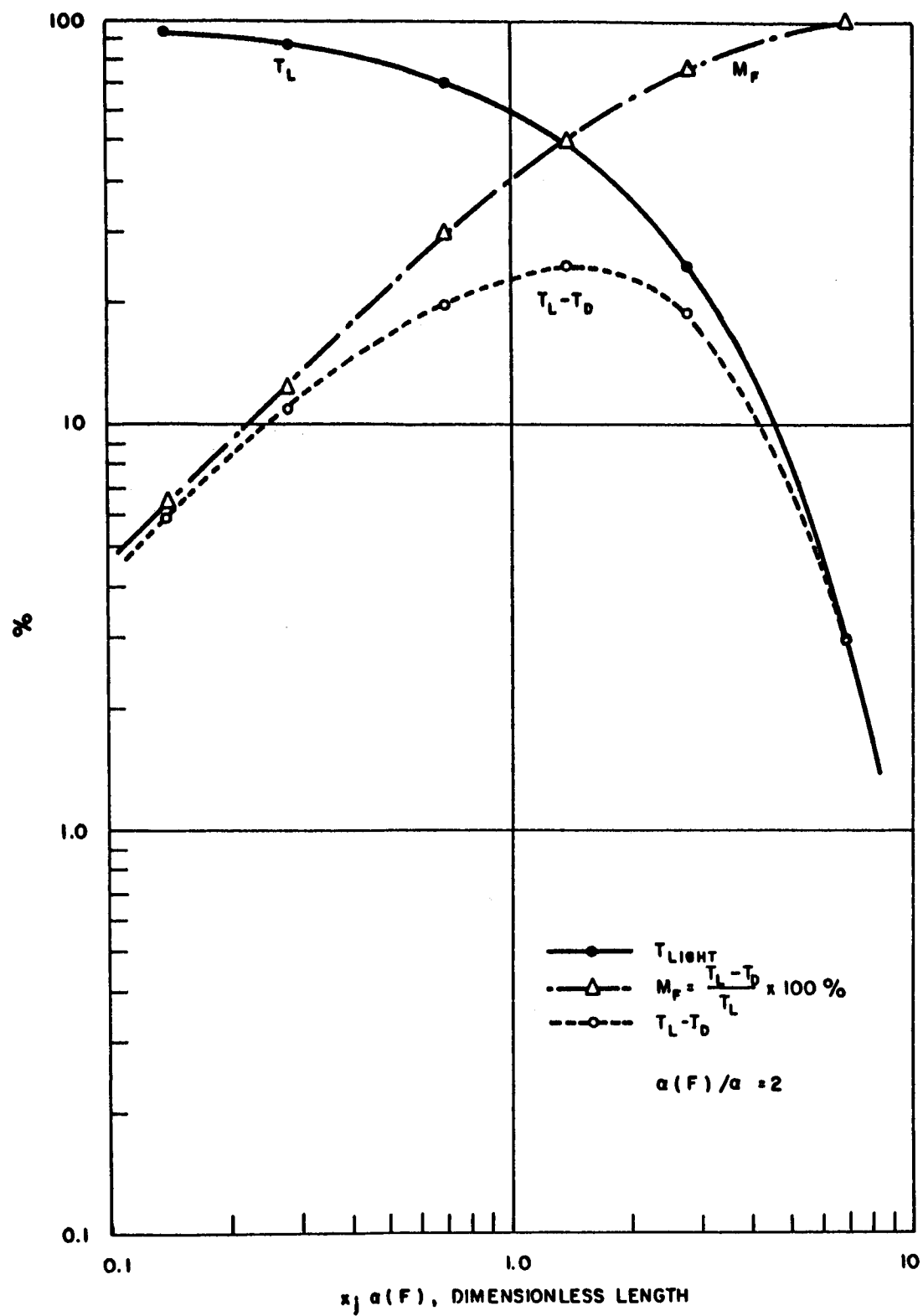


Figure 2

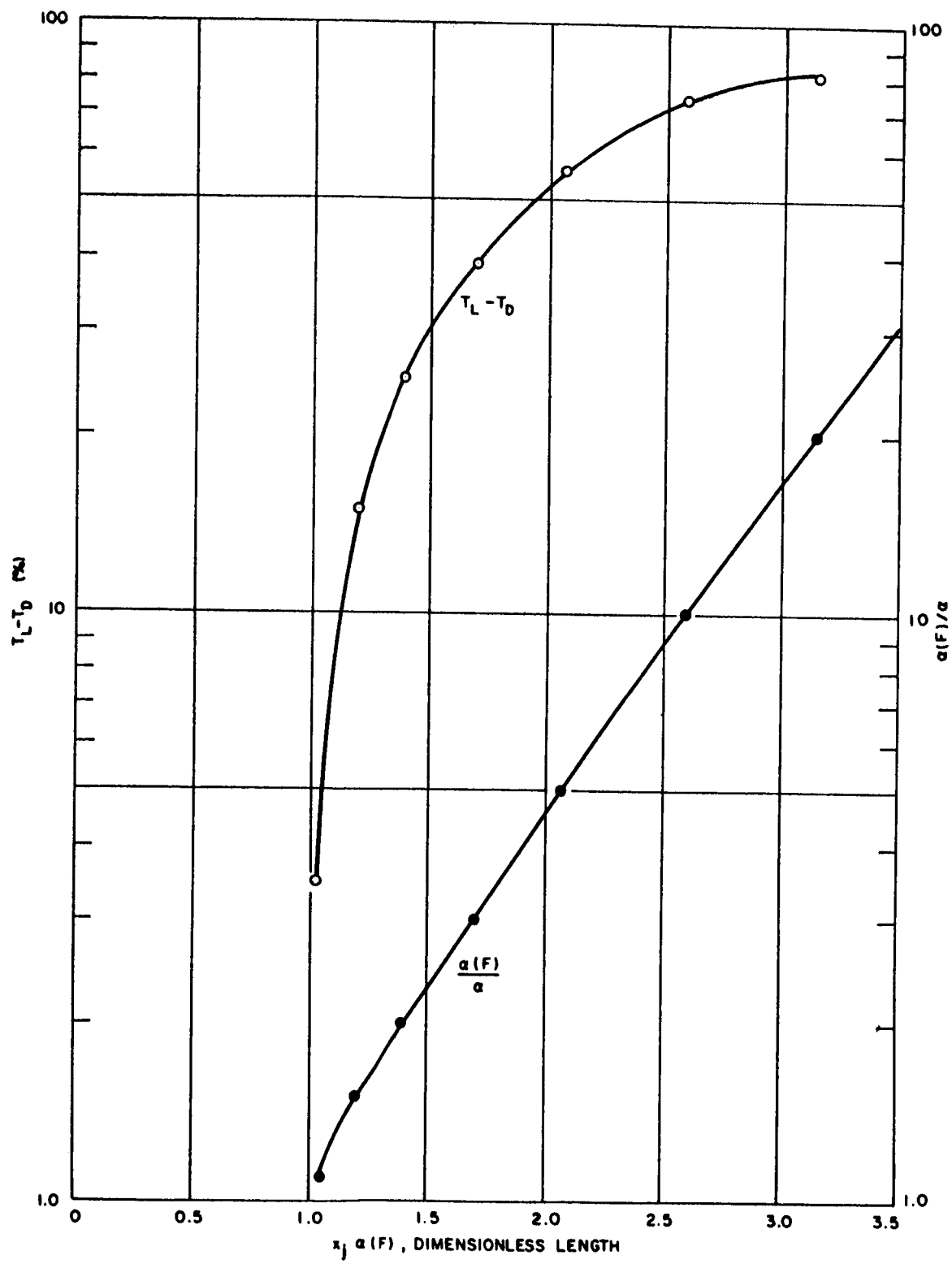


Figure 2

Table IV contains values of $\alpha(F)/\alpha$ as a function of junction doping (and thickness) for InP and GaAs junctions. It also contains values of δE corresponding to the field change.

TABLE IV

Material	Doping	$\alpha(F)$	α	$\alpha(F)/\alpha$	δE
InP	10^{14}	10^4	9.2×10^3	1.02	2×10^{-4}
	10^{15}	10^4	7.7×10^3	1.30	2×10^{-3}
	10^{16}	10^4	7.2×10^2	13.9	2×10^{-2}
	10^{17}	10^4		10^{10}	2×10^{-1}
GaAs	10^{14}	3×10^2	2.96×10^3	1.01	10^{-4}
	10^{15}	3×10^3	2.72×10^3	1.10	10^{-3}
	10^{16}	3×10^3	1.10×10^3	2.72	10^{-2}
	10^{17}	3×10^3		2.2×10^4	10^{-1}

Therefore, InP doped at about 10^{16} or slightly greater would appear most promising. For 10^{16} doping $X_j \left(\frac{1}{\alpha_F} \right) = 0.3$, whereas the optimum positioning requires a value of about 2.85. However,

$$\begin{aligned}
 100\% \left(\frac{T_L - T_D}{I_0} \right) &= e^{-7.2 \times 10^2 \times 3 \times 10^{-5}} - e^{-10^4 \times 3 \times 10^{-5}} \\
 &= 98\% - 74\% = 24\% ,
 \end{aligned}$$

with a modulation index of 25.5%.

Absorption edge data for n and p-type GaAs have recently been published.¹ For a photon energy of 1.40 ev, the published data show that the absorption constant for n-type material doped between 2.5×10^{17} and 3×10^{18} is of the order of 80 cm^{-1} , whereas for p-type material doped at 3×10^{16} , the data show a value of about 700 cm^{-1} . For a δE shift at about 0.1 ev, the p-type absorption constant would be increased to approximately $3 \times 10^3 \text{ cm}^{-1}$. Thus, for a $p^- - n^+$ junction in which the junction field resides in the p^- region, a change of α by a factor of 4 may be expected. This change would produce a maximum value of 7 percent for

$$\left(\frac{T_L - T_D}{I_0} \right) \times 100\%, \text{ and a maximum}$$

modulation index of 8 percent.

These new data corroborate the proposed technique of cross-modulation. Although the value of modulation index is lower than that previously estimated, it is considered good in comparison to most double photon schemes and worthy of further investigations. Experimentally, the problem resolves into one of producing the desired function in configurations of the size envisioned for MIROS applications. Such system considerations will be postponed until later in the program.

1. Braunstein, R., Pankove, J., and Nelson, H., Appl. Phys. Letters 3, 31 (1963).

APPENDIX IV

FREE CARRIER ABSORPTION

In 1959 an electronic infrared imaging system was designed and constructed by members of the Philco Research Laboratories.¹ This system was based on the principle of alteration of absorption of infrared light by alteration of free carrier density in a silicon filter. In this apparatus an electron gun provided a beam of electrons which could be scanned to provide a raster at the silicon. Penetration of the electrons into the silicon allowed hole-electron pairs to be generated in sufficient quantity to allow appreciable free carrier absorption of infrared radiation incident at the location of the electron beam impact spot. Display of the detector signal on an oscilloscope proved the device an effective IR scanning system. In Philco Proposal R63-7 concerning the MIROS study program, it was suggested that the same principle of free carrier absorption could be used for the proposed cross-modulation application in which the free carrier injection would be accomplished by one of the light beams. A review of the published literature^{2, 3, 4} has disclosed some analytical and experimental information on the subject, including a very timely effort⁴ to produce modulation by this technique.

In the McQuistan and Schultz work, carriers were injected electrically, using broad-area junctions of alloyed indium onto germanium. Direct bias current densities of 2 amp/cm² and alternating current densities of about 1.5 amp/cm² were used to control the transmitted light from a Nernst glower at wavelengths of 2 to 12 microns. These authors

1. M. E. Lasser, P. H. Cholet, and R. B. Emmons, "Electronic Scanning System for Infrared Imaging," Proceedings of the IRE, 47, 2069, 1959.
2. R. Desvignes, "Optical Absorption by Free Hole-Electron Pairs Liberated by the Photoelectric Effect in a Germanium Single Crystal," C. R. Acad. Sci (Paris), Vol. 246, No. 12, 1824-7, March 24, 1958.
3. L. Huldt, "Determination of Free Carrier Lifetimes in Semiconductors from the Relaxation Time of Photo-Excited Infrared Absorption," Arkiv for Fysik, 15, 229-36, 1959; also Ark. Fys. 20, 527, 1962.
4. R. B. McQuistan, and J. W. Schultz, "Modulation of Infrared by Free Carrier Absorption," J. Applied Physics, 35, April 1964, p. 1243.

define modulation efficiency as the amplitude of the modulated fundamental of the radiant power normalized to the ideal value of the sinusoidal modulation of all the radiant power incident on the modulator. These efficiencies depend on the minority carrier (hole) lifetime. A modulation index is also defined as a measure of the amplitude of the fundamental of the modulated radiant power normalized with respect to the radiation transmitted when no ac signal is present. This particular figure of merit would be of interest in a MIROS application. Relative modulation index of 10^{-3} to about 0.7 is plotted versus injection current density from 10^{-2} to 10 amp/cm^2 , indicating, as one would conjecture, a linear relationship with increasing carrier concentration (current), and showing very encouraging modulation capabilities at higher levels of operation. These authors showed that relative modulation efficiency versus wavelength increases irregularly from 1.0 to about 1.8 for wavelengths increasing from 2 to 12 microns. The preferred range of operation, according to this curve, is from about 7 to 12 microns. Experimental modulation results show a good fit to an expression derived for the modulation index varying as $(1 + \omega^2 \tau_p^2)^{-1/4}$ for two values of τ_p , minority carrier lifetime of 40 and 0.6 microseconds. Flat responses for these samples are observed to about 2500 and 10^5 cps, respectively. For a given carrier injection current, the modulation efficiency increases with lifetime, while the response falloff frequency decreases.

Huldt's determination of free carrier lifetimes is interesting in the MIROS application because of the similarity in technique. Huldt irradiated a silicon and germanium sample with chopped light from a tungsten source (up to 4800 cps) and observed changes in infrared transmission which was chopped at 13 cps. A slow detector was used and was assumed to measure the mean value of transmitted light over several periods of the chopped carrier injection light. For a germanium sample of 50-ohm/cm, resistivity at 11-microns wavelength, a hole lifetime of 165 microseconds was deduced from the data. A curve of transmittance versus chopping frequency shows a falloff at about 300 cps in agreement with theory developed by Huldt and in the McQuistan and Schultz paper.

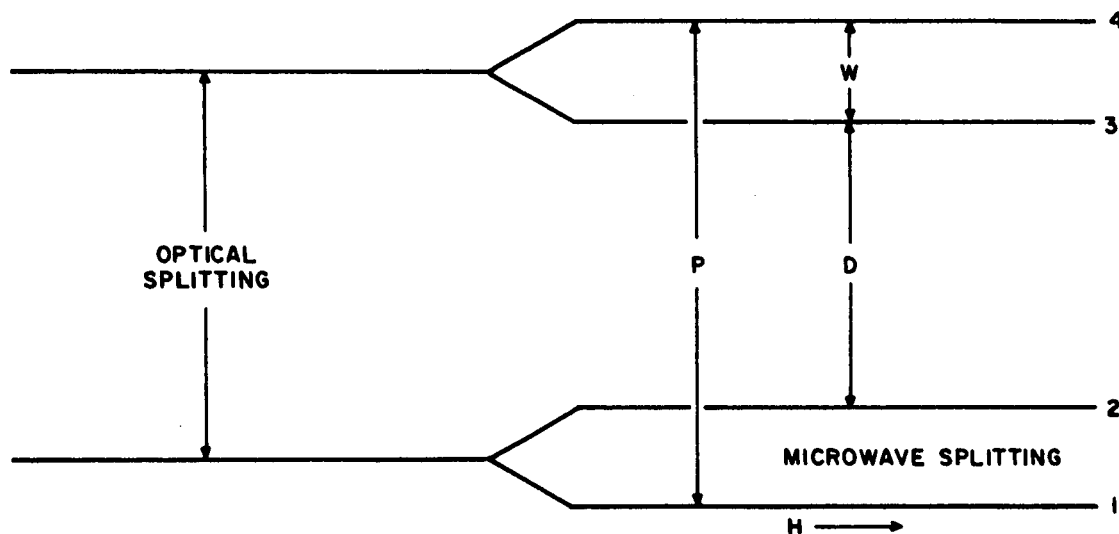
In the production of free carriers by low energy photons, one would assume that perfect efficiency would provide one pair per photon, in contrast to the estimated 2000 pairs per high energy electron in the infrared scanner of Lasser, Cholet and Emmons. These authors used a blanking spot area on silicon of about $3 \times 10^{-4} \text{ cm}^2$ and 0.5 ma current at 25 KV. An equivalent photon flux would be of the order of 10^{22} photons/ $\text{cm}^2\text{-sec}$ or a few kilowatt/ cm^2 power densities at the wavelengths of interest. With laser sources in the laboratory, this value of light flux is

easily attainable, and the substitution of a laser beam for the electron beam in the infrared scanner is a logical suggestion. However, transmission of power of this magnitude to a satellite at long distances in other than short pulses requires lasers of far greater capacity than presently available. One, therefore, is forced to conclude that the concept of cross-modulating using free carrier absorption is practicable in the laboratory, where high photon fluxes are possible, but virtually impossible in CW operation for long distance satellite optical communications work.

APPENDIX V

THEORETICAL DISCUSSION OF OPTICAL PUMPING*

The following model is used for the optical pumping cross modulation effect. We assume a system of atoms with four energy levels which correspond to the hyperfine splitting in the ground and first excited states of the alkali metal vapor atoms.



Optical transitions are excited between levels 1 and 4 by light of one sense of circular polarization at a rate P per sec per atom. Light of the opposite sense of circular polarization is assumed to cause transitions between levels 3 and 2. We assume that spontaneous emission from the excited states (3, 4) occurs very rapidly and with the same probability $w \text{ sec}^{-1}$ to each ground state.

We assume that the upper states 4, 3 thermalize very rapidly at rate W . The ground states are assumed to thermalize slowly at a rate $1/\tau$. Let n_i be the population of each level i . The following equations now apply to this model.

* Analysis by Dr. D. L. Carter of the Physics Department, University of Pennsylvania, part-time consultant to Philco Research Division during the contract period.

$$\left\{ \begin{array}{l} n_1 + n_2 + n_3 + n_4 = N \text{ total number} \\ dn_2/dt = -n_2 (D + 1/\tau) + n_1 (1/\tau) + n_3 w + n_4 w \\ dn_1/dt = n_2 (1/\tau) - n_1 (P + 1/\tau) + n_3 w + w n_4 \\ dn_3/dt = n_2 D - n_3 (W + 2w) + n_4 W. \end{array} \right\} \quad I$$

The equations are solved under the following conditions $w, W \gg (1/\tau)$, P, D . P is assumed to vary with time as $P(t) = P(1 + k e^{i\omega_M t})$, an amplitude modulation at frequency ω_M with fractional modulation, k . The equations are linearized. $n_i = n_i^0 + x_i e^{i\omega_M t}$ where n_i^0 is the population of the i^{th} state when $k = 0$, x_i is the (complex) amplitude of the time varying part of n_i . $dn_i/dt = i\omega x_i e^{i\omega_M t}$. The equations must hold for all times t . Thus an equation like

$$\begin{aligned} i\omega x_i e^{i\omega t} = & - (n_1^0 + x_1 e^{i\omega_M t}) \left[P(1 + k e^{i\omega_M t}) + 1/\tau \right] + (n_2^0 + x_2 e^{i\omega_M t}) 1/\tau \\ & + (n_3^0 + x_3 e^{i\omega_M t}) w + (n_4^0 + x_4 e^{i\omega_M t}) w \end{aligned}$$

must separate into a time varying part

$$i\omega x_1 = -x_1 (P + 1/\tau) + x_2 1/\tau + x_3 w + x_4 w - n_1^0 k P$$

and a time independent part

$$0 = -n_1^0 (P + 1/\tau) + n_2^0 1/\tau + n_3^0 w + n_4^0 w.$$

We have excluded terms like $e^{2i\omega_M t}$ because they are small. Thus, for the time independent part, there are a set of equations like I with all the $dn_i/dt's = 0$; and

$$n_1^0 + n_2^0 + n_3^0 + n_4^0 = N \text{ and } x_1 + x_2 + x_3 + x_4 = 0.$$

The time independent solution is

$$n_1^0 = \frac{N (D + 2/\tau)}{P + D + 4/\tau} \quad \text{for } \frac{w}{D}, \frac{w}{P}, w\tau \gg 1.$$

$$n_3^0 = n_4^0 \simeq 0 \text{ and } n_2^0 = N - n_1^0.$$

This is an expected physical result as we can pump at rates much smaller than the spontaneous rate $\sim 10^{-9}, 10^{-10}$ sec. If $P \gg D$ or $1/\tau$ (but still $\ll w$) $n_1^0 \rightarrow 0$ and $n_2^0 \rightarrow N$, i. e., we get optical pumping.

With the n_1^0 determined above we now use it in the time varying part of the equations to get the x_i . The result of calculation is

$$x_1 + x_2 \simeq 0 \text{ to order } \frac{1}{w\tau}$$

$$x_2 = \frac{n_1^0 k P}{(D + P + 4/\tau) + 2 i \omega_M}$$

The number of atoms in state 2 is then

$$n_2 = \frac{N (P + 2/\tau)}{P + D + 4/\tau} \left[1 + k \frac{P (D + 2/\tau)}{(P + 2/\tau)} \frac{\cos (\omega_M t - \theta)}{\{(P + D + 4/\tau)^2 + 4\omega_M^2\}^{1/2}} \right]$$

when we take the real part. θ is the phase shift $\theta = \tan^{-1} \frac{2\omega_M}{D + P + 4/\tau}$.

The light signal in the depump beam is proportional to $Dn_2 \equiv S$. The signal for $P = D \gg 1/\tau$

$$S = \frac{NP}{2} \left[1 + \frac{kP}{2} \frac{\cos(\omega_M t - \theta)}{\{P^2 + \omega_M^2\}^{1/2}} \right]$$

is picked up on the originally unmodulated beam.

For $P \gg \omega_M$ ($P = D$)

$$S = \frac{NP}{2} \left[1 + \frac{k}{2} \cos \omega_M t \right] .$$

The fractional modulation is 1/2 of the input modulation. It is clear from this analysis that a severe reduction in amplitude will occur for conditions $P \ll \omega_M$. In that region

$$S = \frac{NP}{2} \left[1 + \frac{kP}{2\omega_M} \cos(\omega_M t - \theta) \right] \text{ and } \theta \rightarrow 90^\circ .$$

One very important restriction on this type of cross modulation is then: one must have pumping rates at least equal to the modulation frequency for efficient cross modulation.

If $D \ll P$

$$S = ND \left[1 + k \frac{D}{P} \cos \omega_M t \right] \text{ assuming } P \gg \omega_M$$

so that a degradation will occur for a small depumping rate. If $D \gg P \gg 1/\tau$

$$S = NP \left[1 + k \cos \omega_M t \right] ,$$

showing that the signal level is independent of the depumping intensity for high depumping intensity, and the fractional modulation is the same as the input.

DISTRIBUTION LIST

R. H. Chase
Code RET
NASA Headquarters
Washington, D. C. 20546
(2 copies)

Dr. H. H. Harrison
Code RRE
NASA Headquarters
Washington, D. C. 20546
(1 copy)

Mr. A. M. Greg Andrus
Code FC
NASA Headquarters
Washington, D. C. 20546
(1 copy)

NASA Scientific & Technical Information Facility
4833 Rugby Avenue
Bethesda Md. 20014
(13 copies)

Dr. H. H. Plotkin
Code 524
Goddard Space Flight Center
Greenbelt, Md. 20771
(2 copies)

Mr. J. C. Taylor
Code M-ASTR
Marshall Space Flight Center
Huntsville, Alabama 35812
(2 copies)

Dr. W. H. Wells
Code 333
Jet Propulsion Labs.
Pasadena, Calif. 91103
(1 copy)

Mr. H. M. Lawrence
Code TBO
Langley Research Center
Langley Station
Hampton, Va. 23365
(2 copies)

Mr. D. Matulka
AFAL (AVWC)
Wright-Patterson AFB
Ohio 45433
(1 copy)

Mr. W. H. Thompson
Code IIE
Manned Spacecraft Center
Houston, Texas 77001
(1 copy)